Environment Canada | Environnement Canada

National Hydrology Research Institute

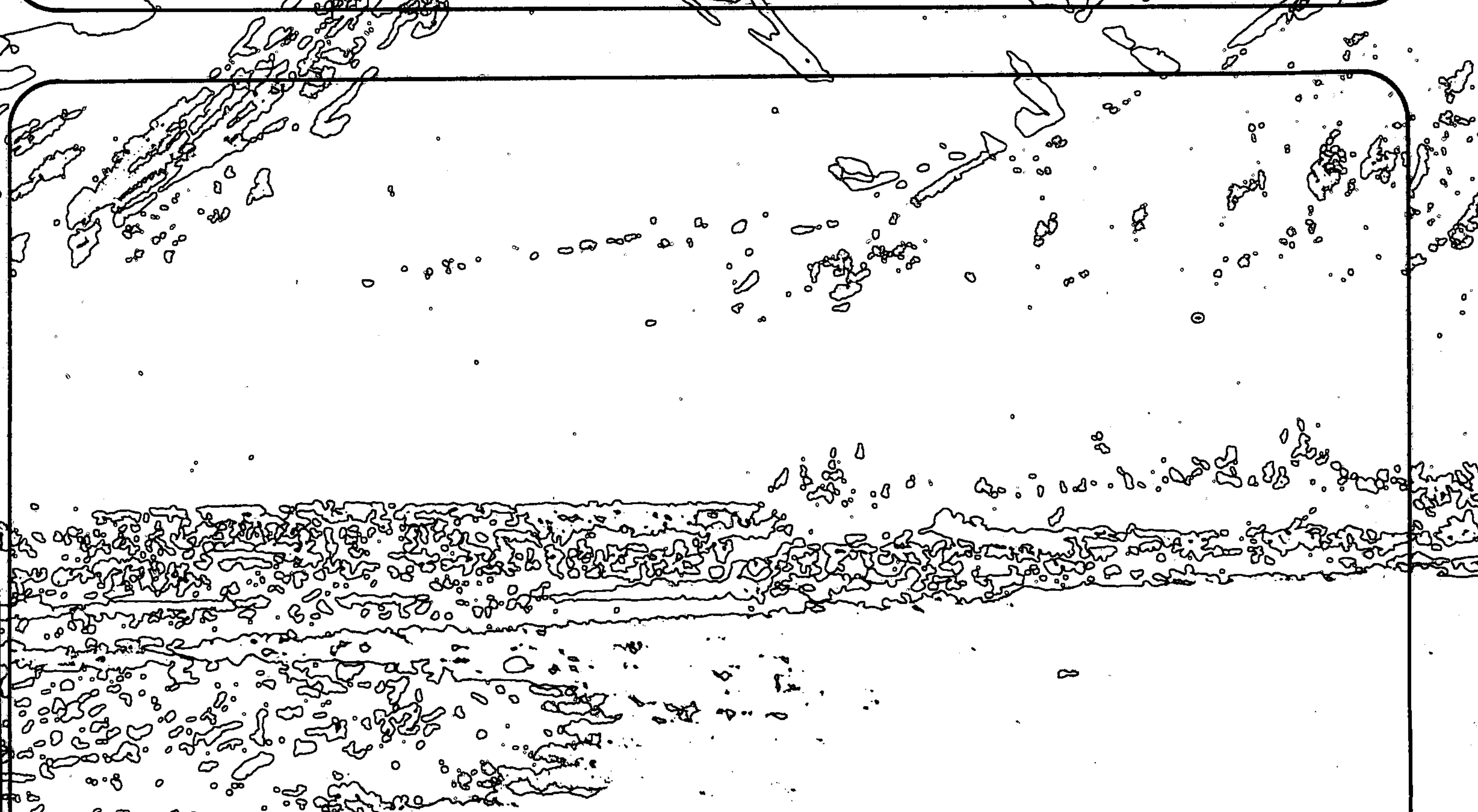

NHRI PAPER NO. 34
IWD SCIENTIFIC SERIES NO. 155

Observations on Ice Cover and Streamflow in the Yukon River near Whitehorse during 1984/85

M.E. Alford and E.C. Carmack

NHRI

INLAND WATERS/LANDS DIRECTORATE
NATIONAL HYDROLOGY RESEARCH INSTITUTE
NATIONAL HYDROLOGY RESEARCH CENTRE
SASKATOON, SASKATCHEWAN, 1987
(Disponible en français sur demande)

Environment Canada
Environnement Canada

National Hydrology Research Institute

NHRI PAPER NO. 34
IWD SCIENTIFIC SERIES NO. 155

Observations on Ice Cover and Streamflow in the Yukon River near Whitehorse during 1984/85

M.E. Alford* and E.C. Carmack†

*Formerly with:
Water Survey of Canada
Water Resources Branch
Inland Waters Directorate
Pacific and Yukon Region
Whitehorse, Yukon Territory

Current address:
Yukon Expeditions
127 Alsek
Whitehorse, Yukon Territory

†Inland Waters Directorate
National Hydrology Research Institute
National Hydrology Research Centre
Saskatoon, Saskatchewan

Current address:
Fisheries and Oceans Canada
Institute of Ocean Sciences
9860 West Saanich Road
Sidney, British Columbia

NHRI

INLAND WATERS/LANDS DIRECTORATE
NATIONAL HYDROLOGY RESEARCH INSTITUTE
NATIONAL HYDROLOGY RESEARCH CENTRE
SASKATOON, SASKATCHEWAN, 1987
(Disponible en français sur demande)

Published by authority of
the Minister of the Environment

Cat. No. En36-502/155E
ISBN 0-662-15613-7

Contents

Tables

Illustrations

Page

Abstract

The objective of the Yukon Ice Seasonality Experiment (YISEX) is to obtain an understanding of physical processes affecting ice cover on northern lake and river systems. Towards this goal, observations of the hydrology and ice regime along a 4.3-km reach of the Yukon River at Whitehorse were initiated during the winter of 1983/84.

A report is given here of the second year (1984/85) of measurements obtained at the Whitehorse reach. Differences in ice cover evolution (e.g., freeze-up patterns, ice front advance, frazil dam growth, and ripple development) caused by different weather patterns and the effects of specific ice conditions (e.g., core leads, ice fronts, and ice ripples) on the distribution of velocity are discussed. A summary comparison of the two winters is presented.

Résumé

L'objectif de l'Expérience de saisonnalité glacielle du Yukon (ESAGY) est de comprendre les processus physiques qui influent sur la couche de glace à la surface de l'ensemble des lacs et des rivières du Nord. Pour réaliser cet objectif, on a commencé à faire des études de l'hydrologie et du régime des glaces le long d'un bief de 4.3 km du fleuve Yukon à Whitehorse au cours de l'hiver 1983-1984.

Ce rapport porte principalement sur les observations de la seconde année d'étude (1984-1985) du bief de Whitehorse. Nous analysons les différences de l'évolution de la couche de glace (par exemple, régimes de gel, progression des fronts de glace, croissance de barrages de frasil et formation de glaces ondulées). Les différents régimes climatiques et les effets des conditions spécifiques de la glace (par exemple, chenaux non gelés, fronts de glace, ondulations de glace) sur la répartition de l'écoulement sont la cause de ce phénomène. On présente une comparaison sommaire des observations du premier hiver au second.

Observations on Ice Cover and Streamflow in the Yukon River near Whitehorse during 1984/85

M.E. Alford and E.C. Carmack

INTRODUCTION

Objectives

The overall goal of the Yukon Ice Seasonality Experiment (YISEX) is to acquire an overview of processes affecting the seasonal ice cover on rivers and lakes of the Yukon River basin. To this end, a study of the ice regime and hydrology along a 4.3-km reach of the Yukon River near Whitehorse was carried out during the winter of 1983/84 (see Alford and Carmack, 1987). This program was extended into a second year with the objective of obtaining a comparison of ice and hydraulic features under different weather patterns.

Here we compare environmental conditions observed in 1983/84 with those of 1984/85 and focus on certain processes that appear to have an important effect on the seasonal ice cycle. Because the winter of 1984/85 was characterized by relatively mild temperatures and higher than average snowfall, the effect of such climatic conditions on the formation of ice could be compared with observations from the previous winter, especially with regard to

(1) the process and pattern of freeze-up, including factors controlling the growth of shore ice;

(2) rates of growth and decay of frazil dams, including changes in their physical properties;

(3) the effects of ice formation and ice front advance on water levels, flow resistance, and vertical profiles of velocity; and

(4) the process and pattern of breakup, including the formation of ripples at the ice/water interface.

Study Area

That part of the Yukon River selected for study extends from the Robert Campbell Bridge at the south end of Whitehorse to the narrows located 4.3 km downstream (Fig. 1). Here, the river drains an area of about 19 400 km^2 and has an annual streamflow of about 240 m^3 s^{-1}. The average slope of the river through the reach is 0.5×10^{-3}.

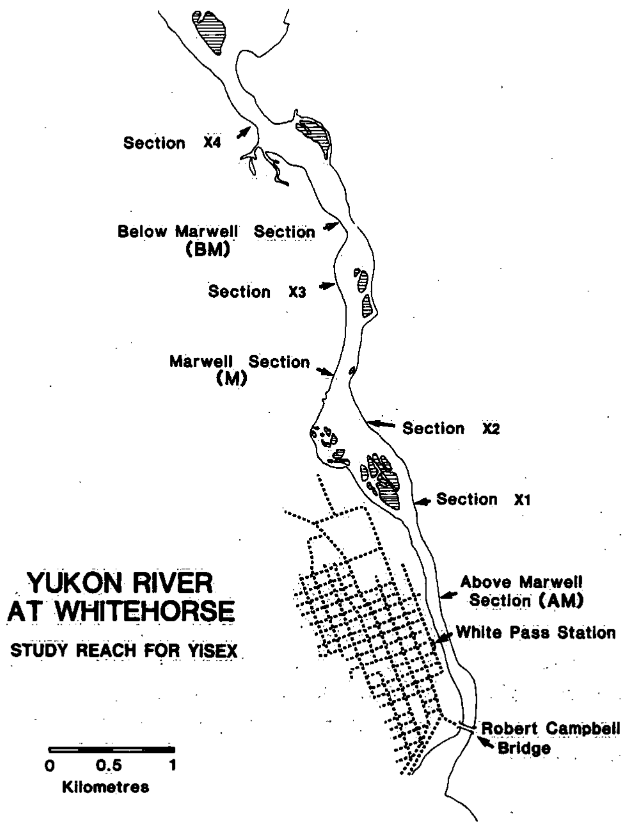

Figure 1. Study area showing station locations.

The flow of the Yukon River has been modified by the construction of two upstream dams. The first, located below the outlet of Marsh Lake, provides some upstream storage. The second, located at Whitehorse Rapids, is a hydroelectric power station. At present the streamflow at Whitehorse is regulated at the lower dam, subject to structural and legal limitations. Specifically, water levels behind the dam (Schwatka Lake) cannot rise above 653.34 m or fall below 652.27 m.

Measurements

Water level was recorded daily at four stations during freeze-up and at three stations for the duration of the winter period. The three locations were the same as those used for the 1983/84 program (AM, M, and BM), while the fourth location was at X4. At each of the locations, measurements were obtained of ice thickness and area, frazil accumulation, frazil hardness, and water velocity at various times throughout the winter. To minimize aliasing problems associated with diurnal variations in water level, all readings were taken at approximately the same time each day. Details of the measurement techniques are given in Alford and Carmack (1987).

Daily values of streamflow were obtained as the total amount of water passing the dam as recorded at the Whitehorse Rapids hydro site (also referred to as "generating station" or GS).

Prior to the onset of freezing, water temperatures were obtained at selected sites extending from the generating station to BM using an expanded-scale mercury thermometer accurate to $\pm 0.1^{\circ}C$.

Air temperature and barometric pressure were recorded at 07:00 at the Alford residence in Riverdale located approximately 1 km from the study reach and within 10 m of river level. We also note that standard meteorological observations, including air temperature, barometric pressure, humidity, wind velocity, and short-wave radiation were recorded at Whitehorse Airport, also located about 1 km from the river, but 61 m above river level. While these data are not reported here, they are obtainable from the Atmospheric Environment Service.

Structural features of the ice were photographed whenever possible. For example, to obtain more detailed information on physical changes that take place on the underside of ice, several blocks were cut using a Swedish ice saw; these were then inverted, spray-painted black, and photographed.

OBSERVATIONS AND COMPARISONS

Meteorology and Hydrology

Comparisons of air temperatures and barometric pressures for the two study years are shown in Figures 2 and 3 respectively. Both winters were milder than normal, however, the winter of 1984/85 was notably warmer than that of the previous year.

A second major difference in meteorological conditions was the higher than average snowfall in 1984/85, especially during the critical months of freeze-up. This is important because snow acts as an insulator, and generally slows the rate of ice growth.

A comparison of streamflow for the two study years (Fig. 4) shows two differences: the flow during 1984/85 was both higher (about 10%) and more variable than the previous year. Since flow can be controlled within narrow limits by the dam at Whitehorse Rapids, any adjustments

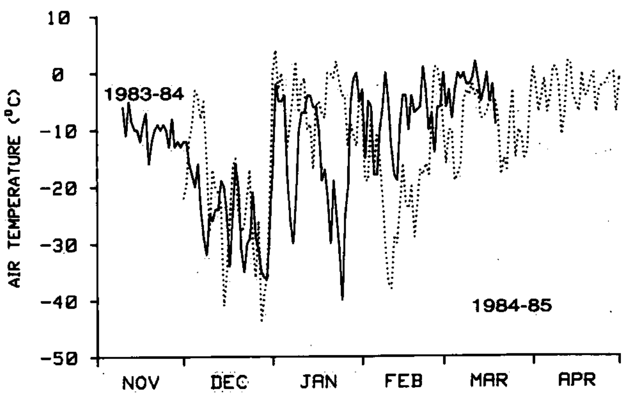

Figure 2. Air temperatures (1983/84 and 1984/85).

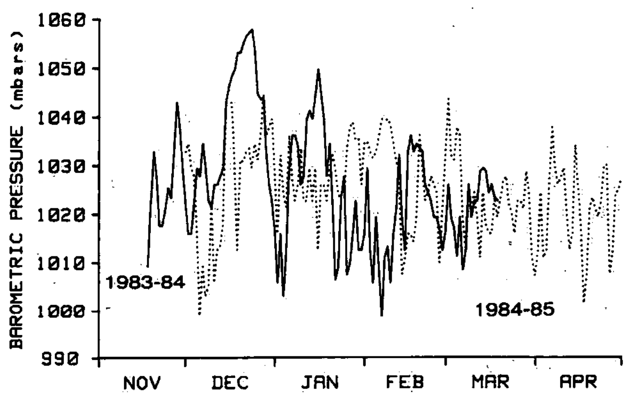

Figure 3. Barometric pressures (1983/84 and 1984/85).

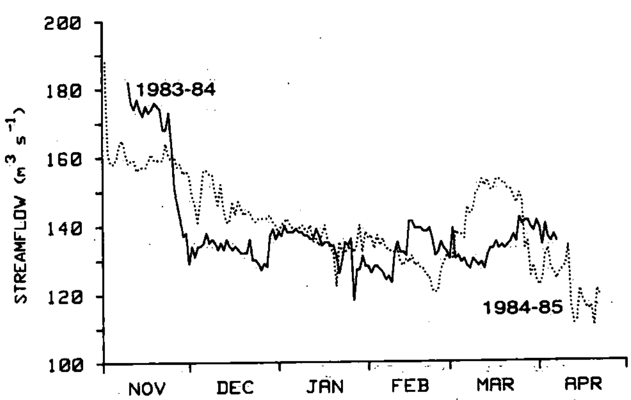

Figure 4. Streamflow (1983/84 and 1984/85).

made for the purpose of turbine maintenance, calibration, and switching can result in short-duration fluctuations in streamflow. During 1984/85 a fourth wheel was placed on-line to allow maintenance of the older turbines; the observed fluctuations are likely related to the phase-in of this turbine.

Ice Cover Distribution

The freezing sequence observed in 1984/85 is summarized in Figure 5 (see also Appendix). Shorefast ice began forming in the back channels of the river in early November. By November 9 it lined most of the reach.

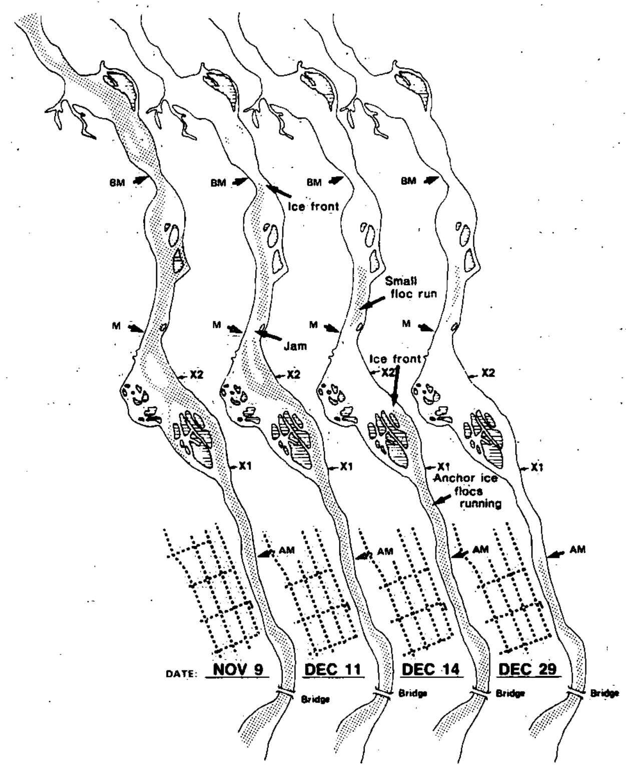

Figure 5. Freezing sequence observed in 1984/85.

The rest of the freeze-up was characterized by a combination of shore ice closing in, thus forming a narrow channel along the velocity core, and the progressive advance of an ice front due to the deposition of frazil flocs, pans, and floes formed farther upstream. On December 11 the ice front moved past BM, and a midchannel jam formed at M. By December 14 the main front had moved to a point midway between X2 and X1. However, a large area of open water remained near M. By December 29 the ice front had progressed upstream from AM. We define freeze-up for this reach as the time the ice front advanced to AM. In 1983/84 the ice front advanced to AM on January 2, roughly the same time as in 1984/85.

Maximum ice coverage occurred between February 12 and March 13. The open lead in the proximity of M remained through most of the winter, not freezing until February 12. Another lead remained in place above the Robert Campbell Bridge throughout the winter. This latter feature has become a common occurrence as the bridge pier initiates the formation of an ice jam on its upstream side. Ice cover invariably extends to the first bend above the bridge, but no farther.

Ice cover conditions during midwinter and spring are shown in Figure 6 (see also Appendix). The first signs of breakup in late March and early April included the appearance of small patches of overflow and the accumulation of pans of broken ice into jams. By April 8 significant thermal leads had appeared along the reach. By April 12 the reach was essentially open, except for a minor jam at BM, and only shore and grounded ice remained. We define breakup for this reach as the time the reach was open to BM. In 1983/84 the reach opened on March 29, approximately two weeks earlier than in 1984/85.

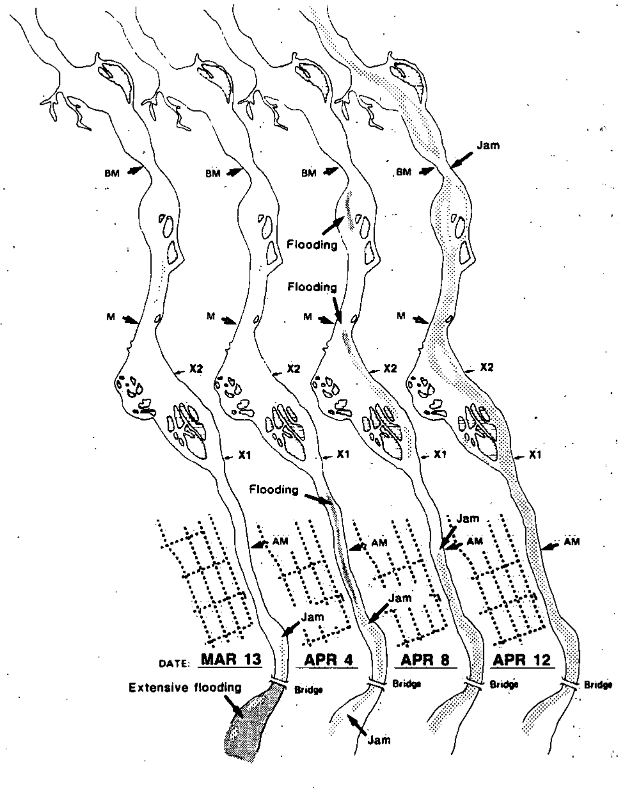

Figure 6. Breakup sequence observed in 1984/85.

Daily values of areal ice cover were computed from the maps shown in the Appendix and are listed in Table 1.

Table 1. Area of Ice Cover

Date	X4 to GS (km²)	X4 to GS (%)	AM to M (km²)	AM to M (%)
84-11-09	0.8542	51.0	0.2857	63.9
84-11-17	0.8987	53.6	0.2889	64.6
84-11-20	0.9255	55.2	0.2944	65.8
84-11-21	0.9326	55.6	0.2944	65.8
84-11-26	0.9554	57.0	0.2970	66.4
84-11-29	0.9862	58.8	0.2983	66.7
84-12-02	0.9989	59.6	0.3049	68.2
84-12-03	1.0215	61.0	0.3096	69.2
84-12-04	1.0289	61.4	0.3128	69.9
84-12-05	1.0568	63.1	0.3148	70.4
84-12-06	1.0575	63.1	0.3154	70.5
84-12-07	1.0920	65.2	0.3170	70.9
84-12-08	1.0920	65.2	0.3170	70.9
84-12-09	1.1388	68.0	0.3185	71.2
84-12-10	1.1408	68.1	0.3237	72.4
84-12-11	1.1414	68.1	0.3284	73.4
84-12-12	1.1440	68.3	0.3289	73.5
84-12-13	1.1472	68.5	0.3318	74.2
84-12-14	1.2159	72.6	0.3849	86.0
84-12-15	1.2192	72.8	0.4018	89.8
84-12-16	1.2298	73.4	0.4026	90.0
84-12-17	1.2387	73.9	0.4051	90.5
84-12-18	1.2387	73.9	0.4051	90.5
84-12-19	1.2684	75.5	0.4195	93.8
84-12-20	1.2648	75.5	0.4195	93.8
84-12-21	1.2648	75.5	0.4195	93.8
84-12-22	1.2769	76.2	0.4259	95.2
84-12-23	1.2769	76.2	0.4259	95.2
84-12-24	1.2801	76.4	0.4305	96.2
84-12-25	1.2960	77.3	0.4336	96.9
84-12-26	1.2982	77.5	0.4341	97.0
84-12-27	1.3018	77.7	0.4380	97.9
84-12-28	1.3057	77.9	0.4387	98.1
84-12-29	1.3060	77.9	0.4410	99.3
84-12-30	1.3224	78.9	0.4457	99.6
84-12-31	1.3236	79.0	0.4464	99.8
85-01-01	1.3372	79.8	0.4465	99.8
85-01-02	1.3430	80.1	0.4465	99.8
85-01-03	1.3430	80.1	0.4465	99.8
85-01-04	1.3487	80.5	0.4466	99.8
85-01-05	1.3487	80.5	0.4466	99.8
85-01-06	1.3487	80.5	0.4466	99.8
85-01-07	1.3487	80.5	0.4466	99.8
85-01-08	1.3487	80.5	0.4466	99.8
85-01-09	1.3632	81.3	0.4466	99.8
85-01-10	1.3632	81.3	0.4466	99.8
85-01-11	1.3653	81.5	0.4467	99.8
85-01-12	1.3653	81.5	0.4467	99.8
85-01-13	1.3653	81.5	0.4467	99.8
85-01-14	1.3654	81.5	0.4467	99.8
85-01-15	1.3690	81.7	0.4467	99.8
85-01-24	1.3697	81.7	0.4468	99.9
85-02-08	1.3758	82.1	0.4468	99.9
85-02-10	1.3788	82.3	0.4468	99.9
85-02-12	1.3811	82.4	0.4468	99.9

Table 1. Continued

Date	X4 to GS (km²)	X4 to GS (%)	AM to M (km²)	AM to M (%)
85-02-25	1.4114	84.2	0.4471	99.9
85-03-03	1.4154	84.5	0.4471	99.9
85-03-13	1.4186	84.7	0.4472	100.0
85-03-15	1.4145	84.4	0.4473	100.0
85-03-21	1.3996	83.5	0.4474	100.0
85-03-22	1.3956	83.3	0.4474	100.0
85-03-26	1.3834	82.5	0.4474	100.0
85-03-29	1.3437	80.2	0.4474	100.0
85-04-01	1.3363	79.7	0.4474	100.0
85-04-04	1.3132	78.4	0.4474	100.0
85-04-05	1.2990	77.5	0.4474	100.0
85-04-06	1.2737	76.0	0.4474	100.0
85-04-07	1.2404	74.0	0.4323	96.6
85-04-08	1.2290	73.3	0.4143	92.6
85-04-09	1.1273	67.3	0.3472	77.6
85-04-10	1.0793	64.4	0.3310	74.0
85-04-11	0.9630	57.5	0.3163	70.7
85-04-12	0.9336	55.7	0.3090	69.1
85-04-13	0.8582	51.2	0.2780	62.1
85-04-16	0.7135	42.6	0.2345	52.4

The corresponding plot of ice cover growth between X4 and GS (Fig. 7) shows a rapid increase in cover early on, followed by a much slower increase later. This pattern is similar to that observed in 1984/85.

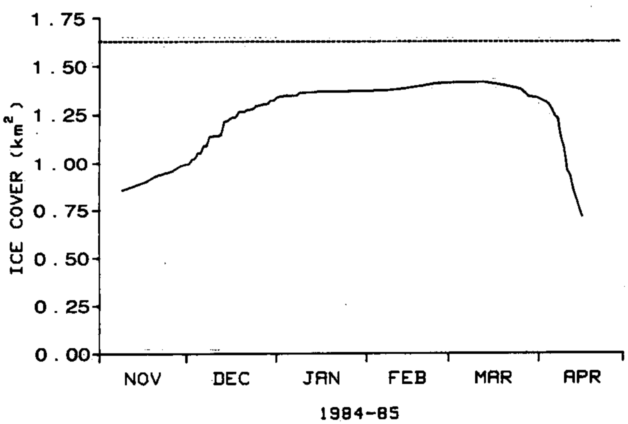

Figure 7. Surface area of ice cover, X4 to GS (November 1984 to April 1985).

Figure 8 and Table 2 show the mean ice thickness at M at six times during the study. Also shown is an estimate of the total volume of surface ice within the reach taken as the product of areal coverage times mean thickness at M. Both curves follow a similar trend with moderate growth during freeze-up, steady conditions in midwinter, and rapid losses at breakup.

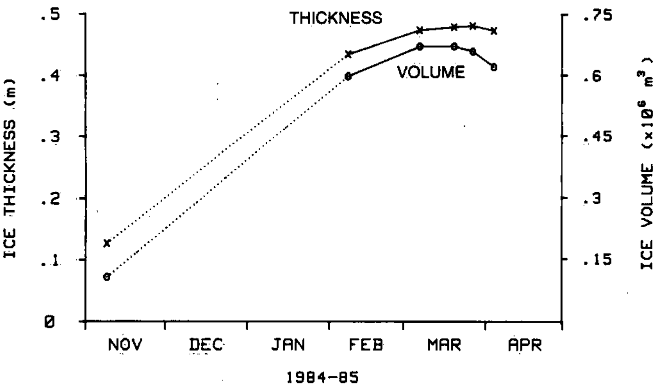

Figure 8. Ice thickness and volume (November 1984 to April 1985).

The ice cover in 1984/85 was about 0.3 m thinner than that observed in 1983/84 as a result of milder temperatures and heavier snow cover.

Table 2. Volume and Thickness of Ice

	Volume (m^3)		Thickness (m)
Date	X4 to GS	AM to M	M
84-11-09	108 244	36 204	0.127
85-02-08	597 097	193 911	0.434
85-03-07	670 099	211 526	0.473
85-03-20	670 204	213 809	0.478
85-03-27	657 696	214 752	0.480
85-04-04	619 830	211 173	0.472

Frazil Dam Characteristics

Frazil dams are defined as mass accumulations of frazil ice particles or slush on the undersides of ice covers. The frazil itself is formed in turbulent, open water areas upstream from the stable ice cover during periods of intense cooling, i.e., at air temperatures of -20°C or colder. (For reviews, see Osterkamp, 1978; Martin, 1981; and Tsang, 1982.) Whether or not frazil adheres at a given location depends upon flow velocity, ice cover roughness, and its own state of "stickiness," determined by whether it is at 0°C or below.

The frazil dam at Whitehorse was discussed by Alford and Carmack (1987). It was noted that the dam appeared to form every year and that the basic shape of the dam was constant from year to year. It was also observed that the cross-sectional area of the dam appeared to reach its limit during the freeze-up period and to decrease thereafter, slowly in midwinter and rapidly just prior to breakup.

Figure 9 shows the ice and frazil horizons observed at M, Figure 10 shows the cross-sectional area of the dam over a period of time. These measurements show a pattern of growth and decay similar to that observed in 1983/84.

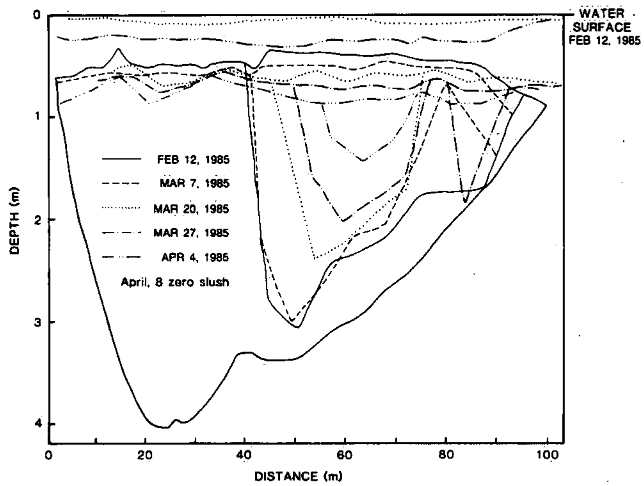

Figure 9. Frazil dam profiles at M (February to April 1985).

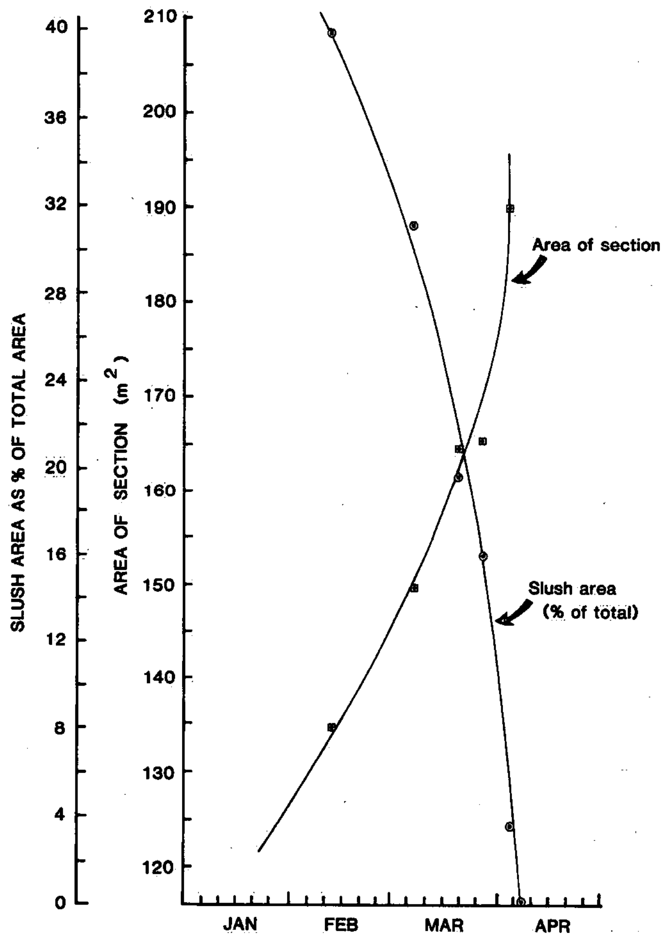

Figure 10. Cross-sectional area of frazil dam at M (January to April 1985).

Additional frazil dam profiles were obtained at AM, X3, BM, and at a section immediately below the open lead at M (Fig. 11). These data show the dam to be continuous along the reach and occupying a volume roughly equal to that of sheet ice. In the middle portion of the reach, slush appears to be absent along the axis of the velocity core. At AM and BM, however, the dam is thickest at midchannel where flow velocities are highest. Our feeling is that when frazil adheres to the ice immediately above the velocity core, and thus acts to divert the flow from its preferred channel, the hydraulic resistance of the reach will be higher than in cases where deposition occurs to the side of the velocity core. This hypothesis, however, requires further study.

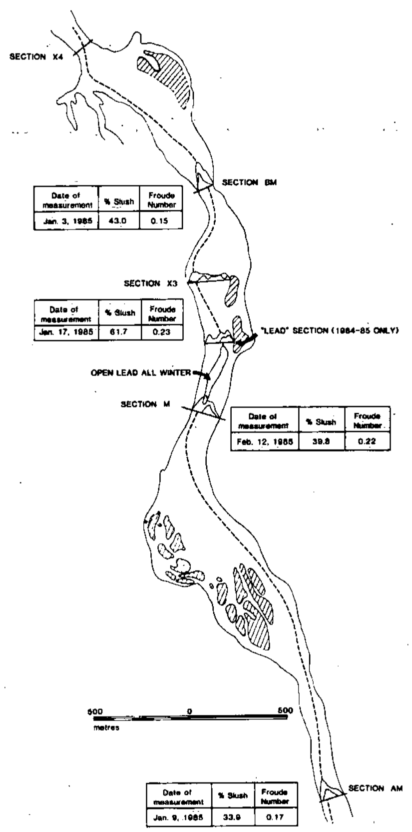

Figure 11. Schematic of frazil dam deposition (1984/85).

Two vertical profiles of frazil dam hardness were taken at BM using a slush rammsonde (Alford and Carmack, 1987). These data (Fig. 12) show a middepth maximum in relative hardness similar to that observed in 1983/84. The morphological reason for this feature is currently unknown.

Hydraulic Conditions

Observations of water level were recorded daily throughout the winter at AM, M, and BM, and for a short

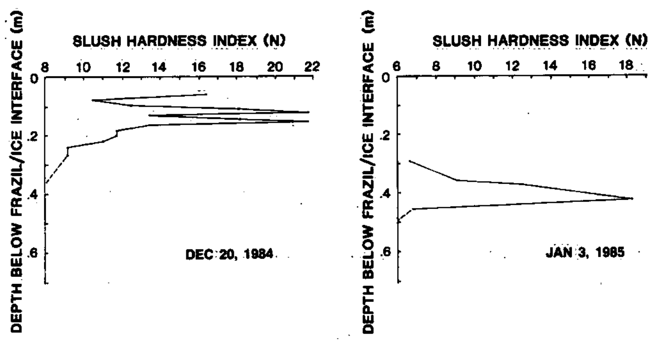

Figure 12. Frazil dam hardness profiles.

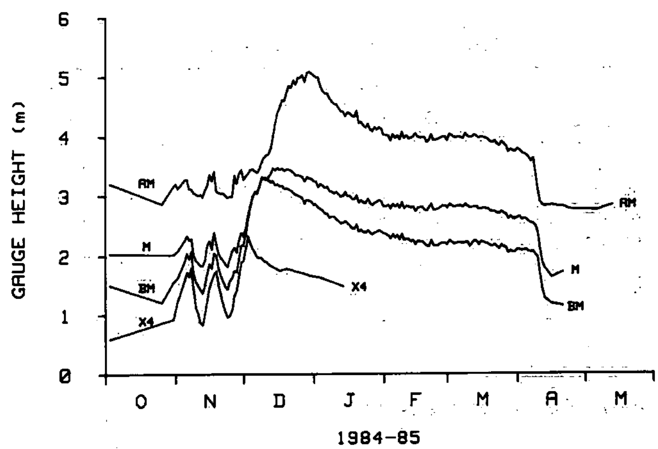

Figure 13. Water levels (October 1984 to May 1985).

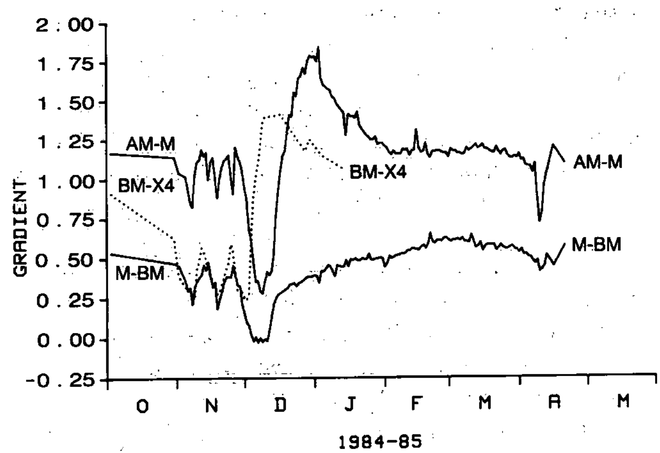

Figure 14. Surface slopes (October 1984 to April 1985).

period during freeze-up at X4. During freeze-up the hydraulic resistance of a river generally increases, requiring a corresponding increase in the depth of flow. Similarly, the overall resistance decreases subsequent to breakup. These effects on resistance are evident from the water level data shown in Figure 13 and Table 3. Water levels at all stations increased rapidly at freeze-up, declined gradually during winter, and fell sharply following breakup. Similarly, observations of surface slope (Fig. 14) reveal significant variations throughout the winter with the largest slopes and most rapid variations occurring at freeze-up. The variation in water level at selected times during the winter cycle is illustrated in Figure 15.

The effect of the advancing ice front on water level (the backwater effect) is shown in Figure 16. Here, the water level at AM is plotted according to the position of the ice front within the reach. Note that a slight backwater effect occurred as the ice front passed BM, and that a much larger effect occurred as the front reached the vicinity of X2. This behaviour is relevant to concerns for flooding.

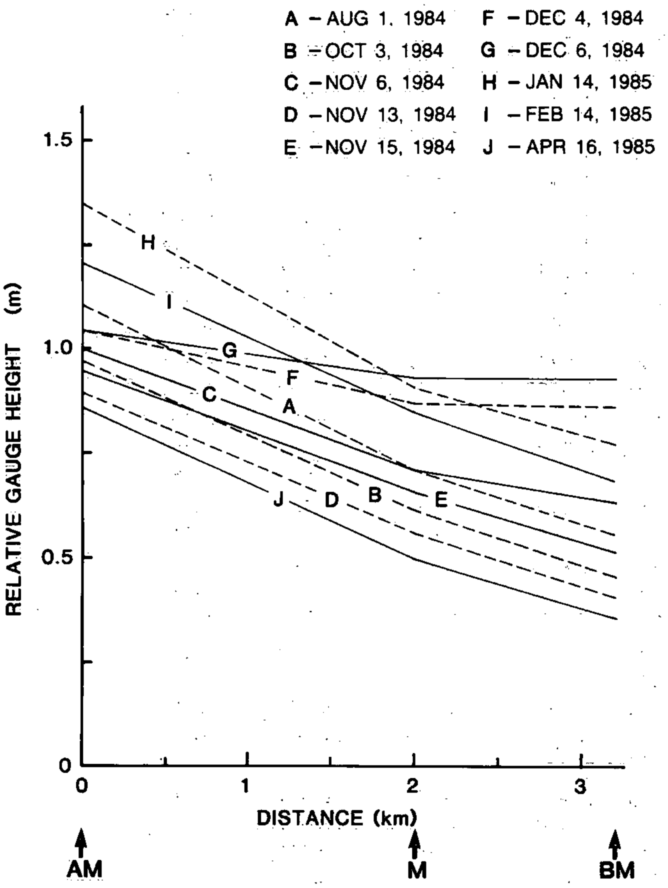

Figure 15. Relative gauge heights at AM, M, and BM at selected times.

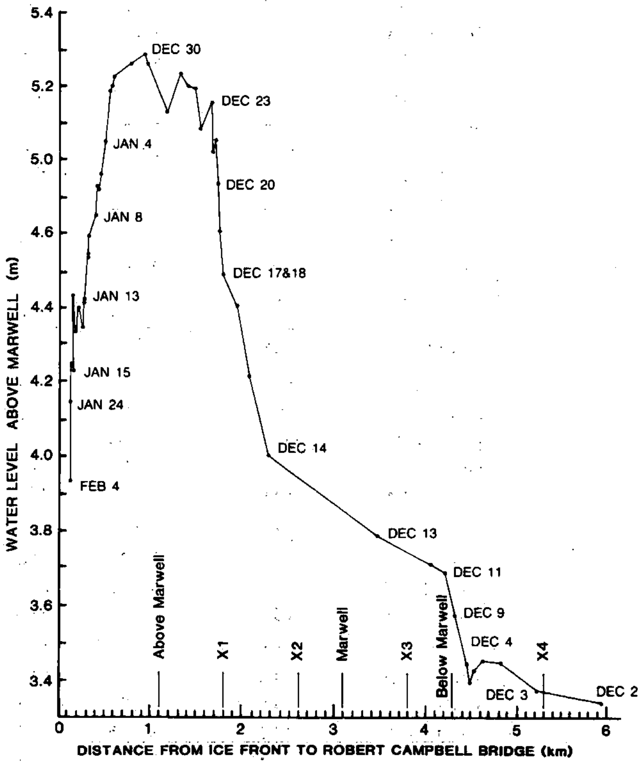

Figure 16. Water level at AM in relation to ice front position.

Table 3. Daily Values of Streamflow, Water Level, and Surface Slope during the Winter of 1984/85

Date	Streamflow ($m^3 s^{-1}$)	Water level				Surface slope		
		AM (m)	M (m)	BM (m)	X4 (m)	AM-M (m)	M-BM (m)	BM-X4 (m)
84-10-03	217	3.200	2.031	1.498	0.590	1.169	0.533	0.908
84-10-26	144	2.860	–	1.207	–	–	–	–
84-10-31	166	3.155	2.015	1.548	0.924	1.140	0.467	0.624
84-11-01	177	3.200	–	–	–	–	–	–
84-11-02	188	3.120	2.080	1.628	1.245	1.040	0.452	0.383

Table 3. Continued

Date	Streamflow ($m^3 s^{-1}$)	Water level				Surface slope		
		AM (m)	M (m)	BM (m)	X4 (m)	AM-M (m)	M-BM (m)	BM-X4 (m)
84-11-05	158	3.270	2.256	1.902	1.585	1.014	0.354	0.317
84-11-06	160	3.276	2.337	2.043	1.722	0.939	0.294	0.321
84-11-07	164	3.120	2.266	1.950	1.648	0.854	0.316	0.302
84-11-08	165	3.110	2.289	2.076	1.800	0.821	0.316	0.302
84-11-09	161	3.050	2.019	1.697	1.445	1.031	0.322	0.252
84-11-10	158	3.030	1.921	1.563	1.130	1.109	0.358	0.433
84-11-11	159	3.000	1.879	1.500	1.020	1.121	0.379	0.480
84-11-12	159	3.020	1.831	1.432	0.865	1.189	0.399	0.567
84-11-13	156	2.980	1.831	1.373	0.830	1.149	0.458	0.543
84-11-14	157	3.102	1.931	1.504	–	1.171	0.427	–
84-11-15	157	3.180	2.182	1.705	–	0.998	0.477	–
84-11-16	157	3.360	2.251	1.866	1.485	1.109	0.385	0.381
84-11-17	159	3.250	2.111	1.791	–	1.139	0.320	–
84-11-18	161	3.410	2.391	2.041	1.695	1.019	0.350	0.346
84-11-19	159	3.080	2.201	2.016	1.740	0.879	0.185	0.276
84-11-20	159	3.050	2.041	1.793	1.510	1.009	0.248	0.283
84-11-21	159	3.040	1.961	1.668	1.340	1.079	0.293	0.328
84-11-22	159	3.045	1.926	1.574	1.185	1.119	0.352	0.389
84-11-23	164	3.000	1.866	1.484	1.055	1.134	0.382	0.429
84-11-24	160	2.970	1.816	1.435	0.960	1.154	0.381	0.475
84-11-25	159	2.990	1.961	1.580	0.990	1.029	0.381	0.590
84-11-26	160	2.990	2.086	1.630	1.090	0.904	0.456	0.540
84-11-27	157	3.345	2.141	1.751	1.330	1.204	0.390	0.421
84-11-28	158	3.210	2.061	1.731	1.430	1.149	0.330	0.301
84-11-29	155	3.380	2.271	1.947	1.660	1.109	0.324	0.287
84-11-30	156	3.440	2.386	2.177	1.890	1.054	0.209	0.287
84-12-01	155	3.275	2.326	2.172	1.925	0.949	0.154	0.247
84-12-02	149	3.330	2.461	2.263	2.125	0.869	0.098	0.238
84-12-03	146	3.375	2.681	2.603	2.330	0.694	0.078	0.273
84-12-04	141	3.440	2.841	2.823	2.210	0.599	0.018	0.613
84-12-05	148	3.450	2.976	2.995	2.118	0.474	-0.019	0.877
84-12-06	156	3.420	3.066	3.059	2.055	0.354	0.007	1.004
84-12-07	156	3.390	3.036	3.062	1.980	0.354	-0.026	1.082
84-12-08	155	3.450	3.156	3.155	1.970	0.294	0.001	1.185
84-12-09	155	3.570	3.291	3.313	1.965	0.279	-0.022	1.348
84-12-10	150	3.650	3.296	3.303	1.910	0.354	-0.007	1.393
84-12-11	146	3.685	3.271	3.288	1.900	0.414	-0.017	1.388
84-12-12	152	3.705	3.311	3.260	1.860	0.394	0.051	1.400
84-12-13	145	3.790	3.371	3.228	1.830	0.419	0.143	1.398
84-12-14	141	4.000	3.461	3.243	–	0.539	0.218	–
84-12-15	141	4.220	3.431	3.178	–	0.789	0.253	–
84-12-16	147	4.400	3.471	3.198	–	0.929	0.273	–
84-12-17	143	4.490	3.441	3.158	1.745	1.049	0.283	1.413
84-12-18	147	4.610	3.461	3.168	–	1.149	0.293	–
84-12-19	145	4.600	3.421	3.118	–	1.170	0.303	–
84-12-20	143	4.740	3.441	3.128	1.780	1.299	0.313	1.348
84-12-21	144	4.850	3.441	3.108	–	1.409	0.333	–
84-12-22	144	4.820	3.421	3.083	–	1.300	0.338	–
84-12-23	142	4.945	3.391	3.048	–	1.554	0.343	–
84-12-24	141	4.870	3.341	3.018	–	1.529	0.323	–
84-12-25	142	4.986	3.341	2.998	–	1.645	0.343	–
84-12-26	142	4.990	3.331	2.983	–	1.659	0.348	–
84-12-27	142	5.030	3.316	2.958	–	1.714	0.358	–
84-12-28	142	4.915	3.241	2.868	1.690	1.674	0.373	1.178
84-12-29	143	5.065	3.311	2.928	–	1.754	0.383	–

Table 3. Continued

Date	Streamflow ($m^3\ s^{-1}$)	Water level				Surface slope		
		AM (m)	M (m)	BM (m)	X4 (m)	AM-M (m)	M-BM (m)	BM-X4 (m)
84-12-30	141	5.085	3.296	2.913	1.660	1.789	0.383	1.253
84-12-31	140	5.060	3.281	2.898	–	1.779	0.383	–
85-01-01	138	5.025	3.241	2.848	–	1.784	0.393	–
85-01-02	140	4.995	3.241	2.854	–	1.754	0.387	–
85-01-03	141	4.984	3.141	2.796	–	1.843	0.345	–
85-01-04	142	4.845	3.196	2.779	1.625	1.649	0.417	1.154
85-01-05	140	4.760	3.161	2.747	–	1.599	0.414	–
85-01-06	139	4.720	3.131	2.700	–	1.589	0.431	–
85-01-07	139	4.725	3.151	2.696	–	1.574	0.455	–
85-01-08	139	4.644	3.076	2.627	–	1.568	0.449	–
85-01-09	140	4.590	3.065	2.647	–	1.525	0.418	–
85-01-10	139	4.545	3.031	2.647	–	1.514	0.384	–
85-01-11	138	4.540	3.061	2.607	–	1.479	0.454	–
85-01-12	140	–	–	–	–	–	–	–
85-01-13	135	4.420	2.981	2.537	–	1.439	0.444	–
85-01-14	136	4.415	2.991	2.544	1.480	1.424	0.447	1.064
85-01-15	134	4.340	2.061	2.574	–	1.279	0.487	–
85-01-16	137	4.400	2.986	2.538	–	1.414	0.448	–
85-01-17	140	4.390	2.991	2.499	–	1.399	0.492	–
85-01-18	136	4.340	2.941	2.455	–	1.399	0.486	–
85-01-19	133	4.330	2.941	2.444	–	1.389	0.497	–
85-01-20	132	4.430	3.001	2.517	–	1.429	0.484	–
85-01-21	122	4.225	2.881	2.399	–	1.344	0.482	–
85-01-22	135	4.240	2.921	2.425	–	1.319	0.496	–
85-01-23	132	4.180	2.881	2.389	–	1.299	0.492	–
85-01-24	132	4.150	2.871	2.378	–	1.279	0.493	–
85-01-25	133	4.210	2.943	2.418	–	1.267	0.525	–
85-01-26	134	4.110	2.861	2.373	–	1.249	0.488	–
85-01-27	132	4.085	2.836	2.348	–	1.249	0.488	–
85-01-28	134	4.150	2.881	2.388	–	1.269	0.493	–
85-01-29	140	4.110	2.891	2.394	–	1.219	0.497	–
85-01-30	132	4.150	2.921	2.419	–	1.229	0.502	–
85-01-31	138	4.120	2.891	2.394	–	1.229	0.497	–
85-02-01	136	4.020	2.811	2.369	–	1.209	0.442	–
85-02-02	137	4.020	2.821	2.355	–	1.199	0.466	–
85-02-03	133	4.010	2.841	2.330	–	1.169	0.511	–
85-02-04	137	3.930	2.776	2.280	–	1.154	0.496	–
85-02-05	134	4.035	2.856	2.350	–	1.179	0.506	–
85-02-06	136	3.970	2.811	2.296	–	1.159	0.515	–
85-02-07	133	4.010	2.851	2.335	–	1.159	0.516	–
85-02-08	133	3.950	2.791	2.266	–	1.159	0.525	–
85-02-09	132	4.070	2.881	2.355	–	1.189	0.526	–
85-02-10	132	3.965	2.781	2.251	–	1.184	0.530	–
85-02-11	133	4.010	2.821	2.276	–	1.189	0.545	–
85-02-12	129	3.960	2.811	2.266	–	1.149	0.545	–
85-02-13	128	3.970	2.791	2.231	–	1.179	0.560	–
85-02-14	130	3.995	2.811	2.256	–	1.184	0.555	–
85-02-15	129	4.045	2.731	2.181	–	1.314	0.550	–
85-02-16	131	3.990	2.791	2.242	–	1.199	0.549	–
85-02-17	128	3.970	2.801	2.231	–	1.169	0.570	–
85-02-18	129	3.980	2.806	2.227	–	1.174	0.579	–
85-02-19	127	3.980	2.751	2.192	–	1.229	0.559	–
85-02-20	127	3.898	2.741	2.152	–	1.157	0.589	–
85-02-21	125	3.935	2.801	2.147	–	1.134	0.654	–
85-02-22	125	4.030	2.856	2.257	–	1.174	0.599	–

Table 3. Continued

Date	Streamflow ($m^3 s^{-1}$)	Water level				Surface slope		
		AM (m)	M (m)	BM (m)	X4 (m)	AM-M (m)	M-BM (m)	BM-X4 (m)
85-02-23	121	3.926	2.753	2.162	–	1.173	0.591	–
85-02-24	120	3.940	2.761	2.152	–	1.179	0.609	–
85-02-25	121	3.950	2.771	2.162	–	1.179	0.609	–
85-02-26	127	3.970	2.801	2.197	–	1.169	0.604	–
85-02-27	129	3.990	2.824	2.202	–	1.166	0.622	–
85-02-28	131	3.990	2.826	2.201	–	1.164	0.625	–
85-03-01	130	3.930	2.791	2.181	–	1.139	0.610	–
85-03-02	138	4.040	2.851	2.250	–	1.189	0.601	–
85-03-03	137	4.010	2.831	2.220	–	1.179	0.611	–
85-03-04	137	3.980	2.801	2.189	–	1.179	0.612	–
85-03-05	136	3.980	2.816	2.199	–	1.164	0.617	–
85-03-06	145	3.990	2.826	2.218	–	1.164	0.608	–
85-03-07	143	3.980	2.826	2.203	–	1.154	0.623	–
85-03-08	144	3.960	2.801	2.197	–	1.159	0.604	–
85-03-09	149	4.050	2.851	–	–	1.199	–	–
85-03-10	150	4.000	2.821	2.225	–	1.179	0.596	–
85-03-11	153	3.980	2.791	2.145	–	1.189	0.646	–
85-03-12	151	3.990	–	–	–	–	–	–
85-03-13	153	4.030	2.811	2.249	–	1.219	0.562	–
85-03-14	150	4.000	2.806	2.233	–	1.194	0.573	–
85-03-15	150	3.970	2.766	2.170	–	1.204	0.596	–
85-03-16	153	3.995	2.776	2.232	–	1.219	0.544	–
85-03-17	153	3.980	2.791	2.221	–	1.189	0.570	–
85-03-18	152	3.970	2.781	2.200	–	1.189	0.581	–
85-03-19	152	3.950	2.771	2.190	–	1.179	0.581	–
85-03-20	150	3.910	2.741	2.160	–	1.169	0.581	–
85-03-21	150	3.895	2.731	2.150	–	1.164	0.581	–
85-03-22	148	3.930	2.726	2.180	–	1.204	0.546	–
85-03-23	146	3.875	2.701	2.140	–	1.174	0.561	–
85-03-24	149	3.845	2.691	2.110	–	1.154	0.581	–
85-03-25	147	3.910	2.731	2.170	–	1.179	0.561	–
85-03-26	133	3.880	2.696	2.140	–	1.184	0.556	–
85-03-27	135	3.835	2.686	2.130	–	1.149	0.556	–
85-03-28	125	3.740	2.606	2.040	–	1.134	0.566	–
85-03-29	128	3.780	2.651	2.078	–	1.129	0.573	–
85-03-30	124	3.750	2.606	2.053	–	1.144	0.553	–
85-03-31	122	3.740	2.606	2.058	–	1.134	0.548	–
85-04-01	124	3.790	2.631	2.098	–	1.159	0.533	–
85-04-02	131	3.770	2.651	2.098	–	1.119	0.553	–
85-04-03	133	3.720	2.596	2.078	–	1.124	0.518	–
85-04-04	127	3.700	2.616	2.093	–	1.084	0.523	–
85-04-05	126	3.680	2.601	2.098	–	1.079	0.503	–
85-04-06	124	3.640	2.561	2.058	–	1.079	0.503	–
85-04-07	126	3.580	2.541	2.063	–	1.039	0.478	–
85-04-08	127	3.630	2.531	2.068	–	1.099	0.463	–
85-04-09	128	3.380	2.491	2.008	–	0.889	0.483	–
85-04-10	134	3.100	2.381	1.969	–	0.719	0.412	–
85-04-11	116	2.890	2.111	1.686	–	0.779	0.425	–
85-04-12	111	2.840	1.881	1.436	–	0.959	0.445	–
85-04-13	112	2.820	1.791	1.276	–	1.029	0.515	–
85-04-16	116	2.840	1.631	1.186	–	1.209	0.445	–
85-04-19	110	2.820	–	–	–	–	–	–
85-04-21	119	2.820	1.721	1.146	–	1.099	0.575	–
85-04-24	–	2.770	–	–	–	–	–	–
85-05-06	–	2.750	–	–	–	–	–	–
85-05-13	–	2.840	–	–	–	–	–	–

OBSERVATIONS OF SPECIFIC PROCESSES

Alford and Carmack (1987) identified several phenomena affecting ice cover development and streamflow within the reach. In the present study, additional observations were made to study certain of these processes in greater detail.

Water Temperature Changes at Freeze-up

Changes in water temperature along the reach at different times during freeze-up are shown in Figure 17. Typically, the temperature changed by about 0.3°C between the bridge and BM, yielding a longitudinal temperature gradient $dT/dL = 0.07°C/km$, where T is water temperature and L is the distance along the reach.

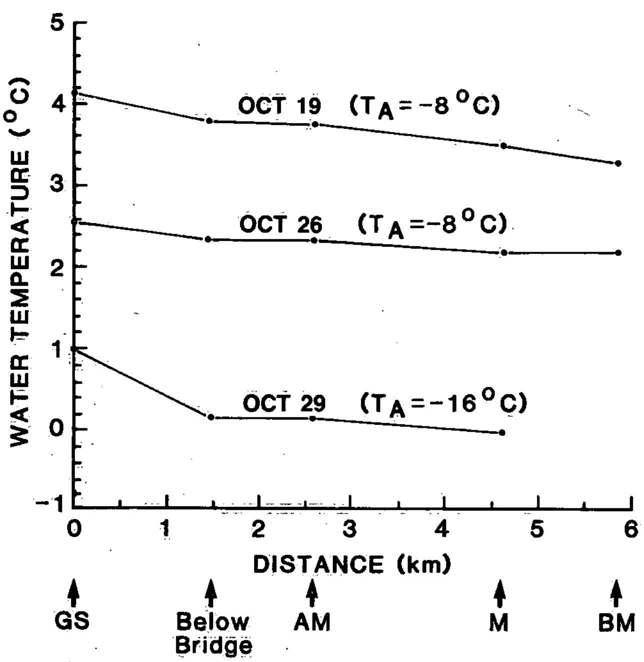

Figure 17. Water temperature gradients prior to freeze-up. (T_A denotes the corresponding air temperature.)

How large must the surface heat flux be to account for the observed longitudinal temperature gradient? Taking the mean velocity $\langle V \rangle = 0.7$ m/s, we note that a column of water moving through the reach cools at a rate of $dT/dt = \langle V \rangle\ dT/dL$, or about 0.5×10^{-4}°C/s. Taking the mean depth of the reach to be 2 m, a surface heat flux of 390 W m^{-2} is obtained. This value should be considered as a rough estimate only, but is in agreement with previous heat flux measurements by Alford and Carmack (1987).

Shore Ice Growth

As noted earlier, the freezing sequence can be characterized as a gradual closing in of shore ice forming a narrow channel along the core velocity, coupled with a progressive advance of the ice front due to the deposition of floes formed farther upstream. This is not to say that the two mechanisms are independent, for the narrower the channel the faster it will fill with drifting ice.

Osterkamp and Gosink (1983) point out that shore ice grows laterally by at least three mechanisms: conductive heat transfer through the ice, accumulation of drifting frazil, and loss of latent heat to supercooled river water. Figure 18 shows shore ice growth by frazil accumulation. Figure 19 shows the presence of dendritic features in the shore ice at a time when the surface heat loss is high and large amounts of frazil are present in the flow.

Because of the existence of the open lead near Marwell, it was convenient to measure the rate of growth of the shore ice coincident with reading of water level. These data (Fig. 20) suggest a strong relationship to air temperature. When plotted as a correlation diagram for the rate of shore ice growth in relation to air temperature (Fig. 21), a simple regression is obtained:

$$dW/dt = AT_a \text{ (in m/day)}$$

where dW/dt = lateral growth of shore ice

T_a = air temperature

A = curve-fitting coefficient applicable (only) to this reach of the river ($A = -0.01$ m/day°C).

Taking the mean temperature at Whitehorse to be about −20°C, one can estimate that shore ice grows at a rate of about 1 m every five days.

Fluctuations in water level also influence shore ice. Observations of shore ice formation were made and sketched to explain some of the reasons why shore ice can be thicker and possibly rougher than the central ice cover (Fig. 22). Other structural features in shore ice, related to shear and the deposition of frazil, are described by Osterkamp and Gosink (1983).

Ice Front Advance

The advance of the ice front through the reach is of prime engineering concern, for it is during this time that the Marwell region of Whitehorse is most prone to flooding.

Figure 18. Shore ice showing diurnal frazil deposit.

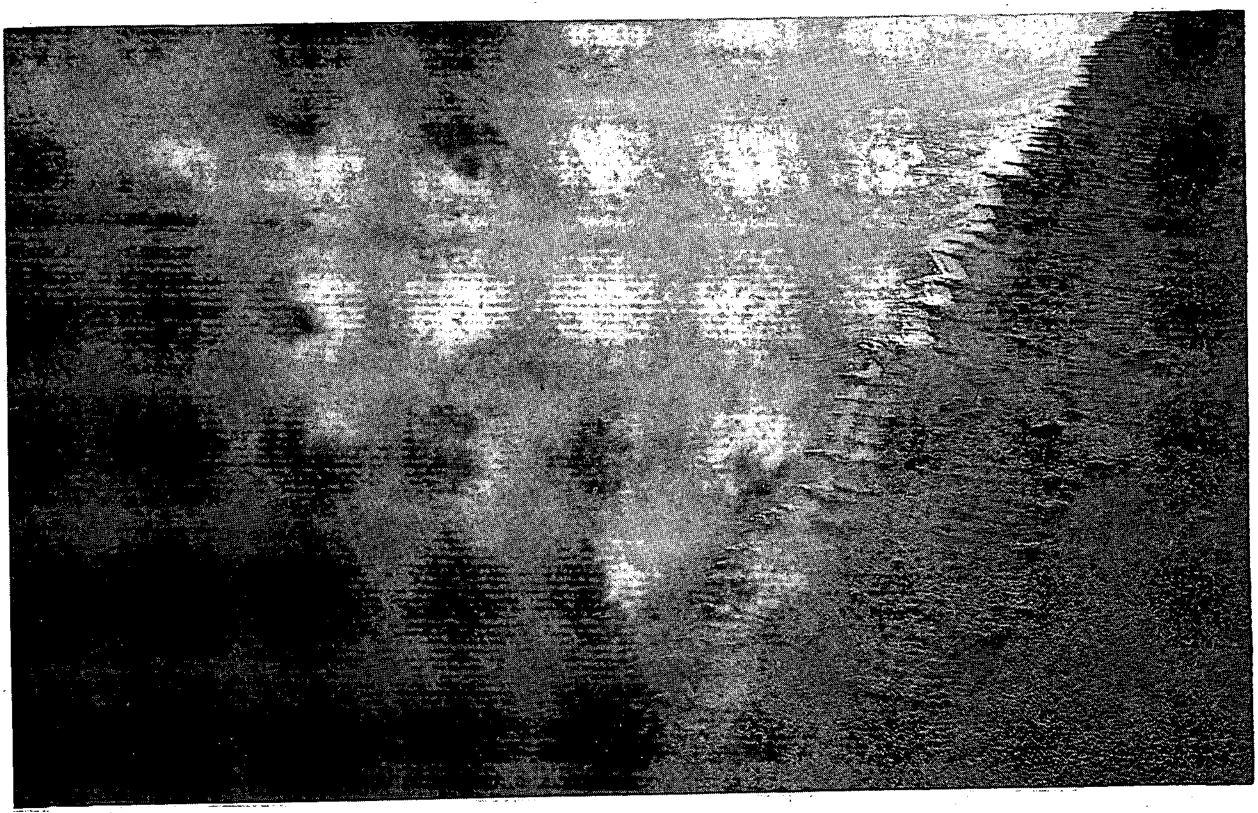

Figure 19. Shore ice showing dendritic features along the edge.

Observations of ice front advance through the reach were made in both 1983/84 and 1984/85 (Fig. 23). From this map it appears that the ice front propagates very quickly from BM to X2, slows between X2 and X1, and moves very slowly above X1. Earlier we noted (Fig. 16) that the backwater effect increases as the ice front passes X2, suggesting that the sensitivity of flooding is related to the speed of ice front advance.

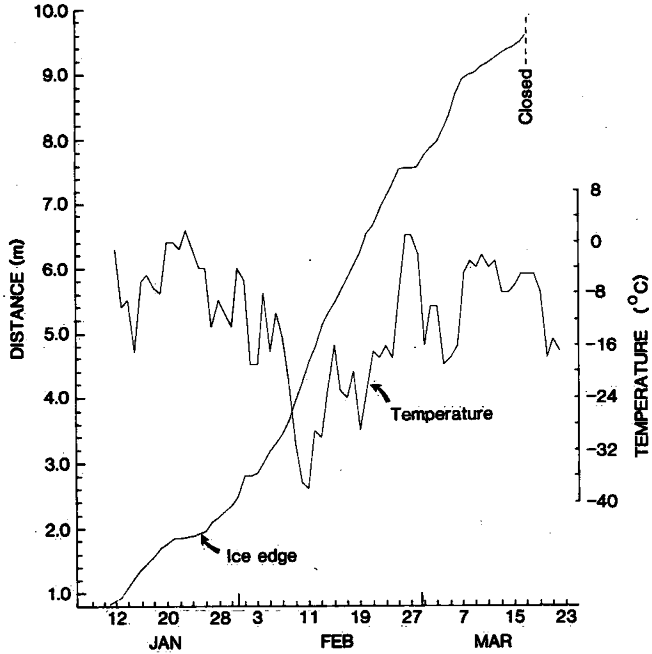

Figure 20. Air temperature and growth of shore ice at open section at M (January to March 1985).

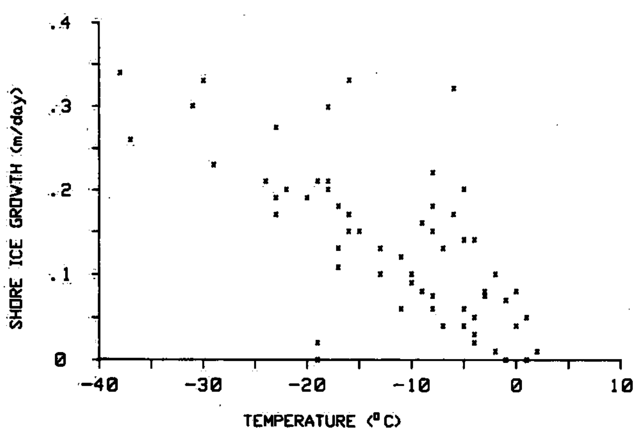

Figure 21. Shore ice growth rate in relation to air temperature.

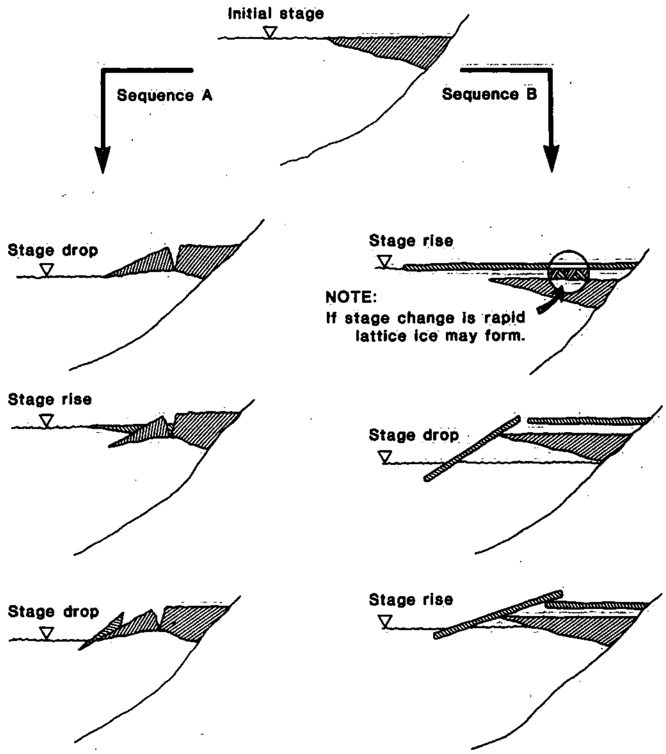

Figure 22. Schematic of structural changes in the growth of shore ice.

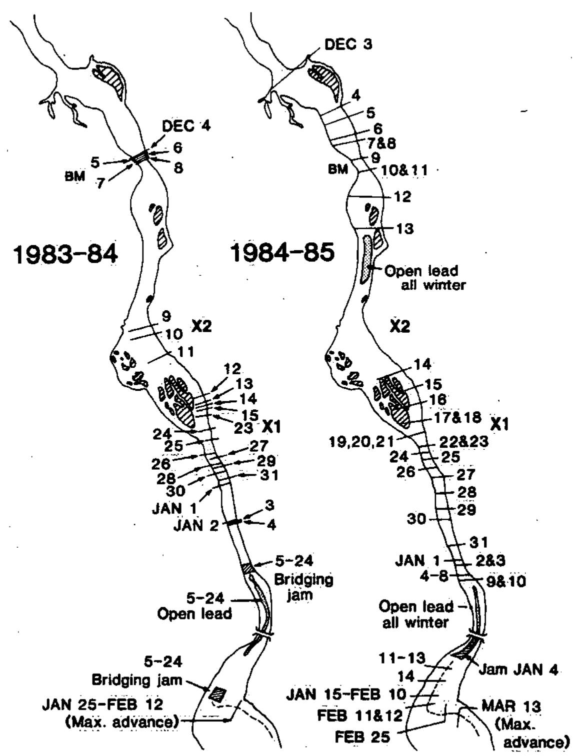

Figure 23. Ice front advance (1983/84 and 1984/85).

Velocity Distributions

Velocity is highly variable in both time and space. The observations described below illustrate how certain hydraulic conditions may alter vertical profiles of velocity.

The existence of an open lead at Marwell allowed us to examine the hydraulic conditions associated with the lead, and to obtain a rough understanding of frazil deposition downstream from the lead.

Vertical profiles of velocity downstream from the lead (Fig. 24) show the progressive establishment of the under-ice boundary layer. At a distance of 5 m from the end of open water the velocity profile is very much like that of an open water profile, with only the upper 0.1 m showing boundary layer development. At 20 m from the edge, however, the profile is much more regular and the boundary layer appears to be fully developed.

A longitudinal section downstream from the open lead (Fig. 25) shows frazil accumulations becoming evident about 8 to 10 m downstream from the open water. At this time the under-ice surface below the lead is quite smooth so that immediate deposition may not be favoured.

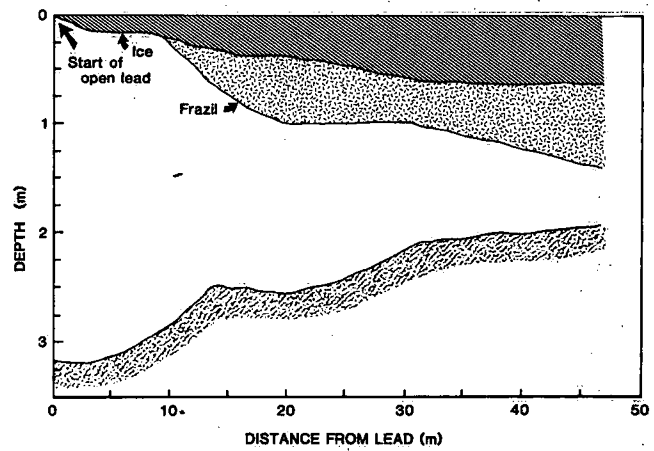

Figure 25. Frazil deposition behind lead.

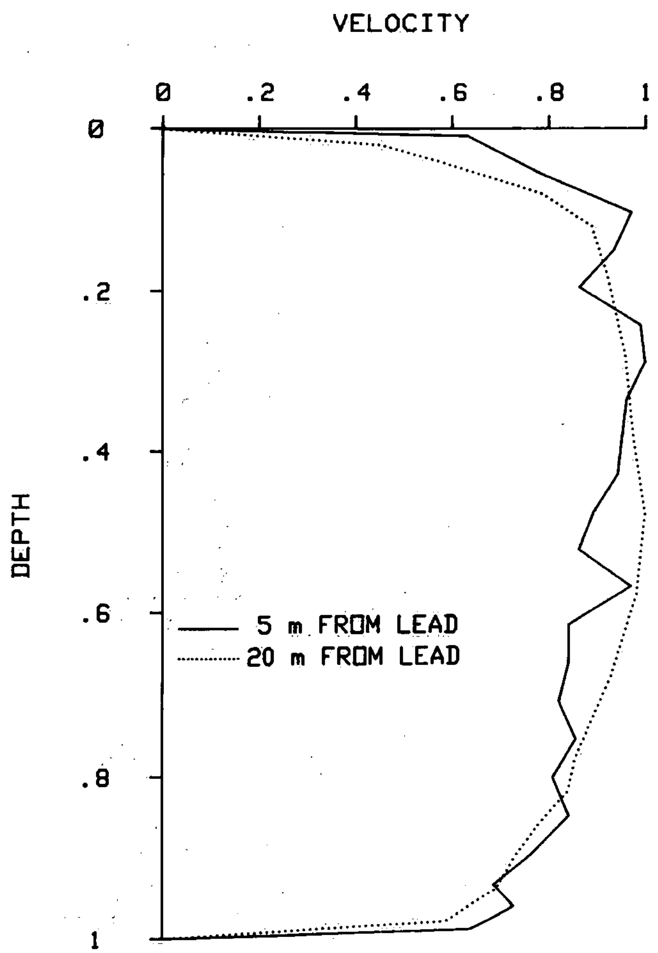

Figure 24. Velocity profiles behind lead.

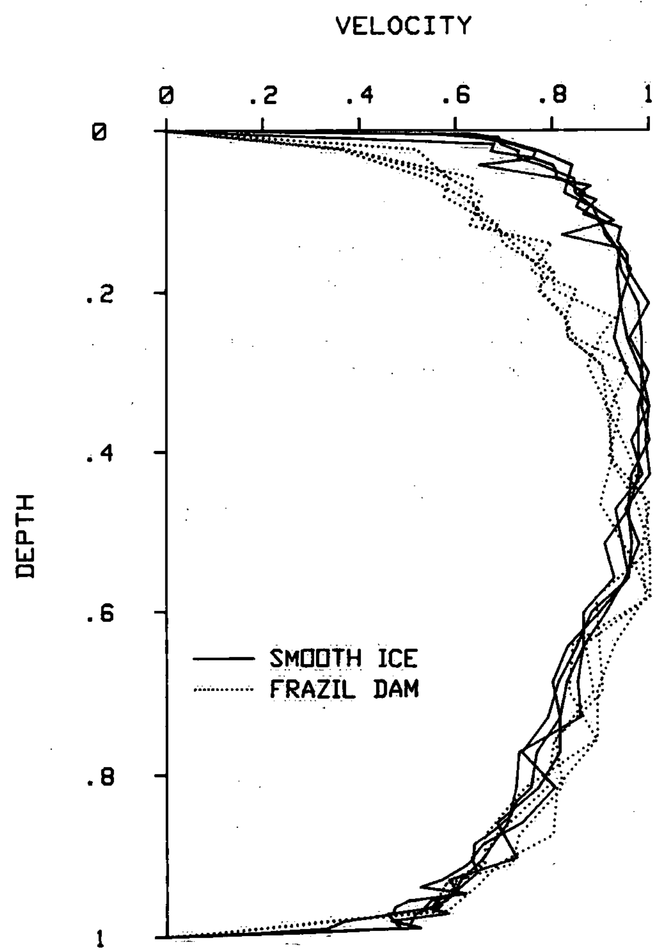

Figure 26. Velocity profiles below smooth ice and below frazil dam.

The presence of a frazil dam may also affect the shape of the velocity profile by presenting a different roughness to the flow. This is supported by the profiles shown in Figure 26 comparing flow under smooth ice with that under a frazil dam. In this case it appears that the friction velocity under the more irregular frazil dam is greater than that under the smooth, surface ice where no frazil is present.

Ice Ripple Formation

With the onset of spring, instabilities in the flow of warm (perhaps 0.02°C) water results in the formation of wavelike features, called ice ripples, at the ice/water interface (Carey, 1966; Ashton and Kennedy, 1972). The fluid mechanics of heat transfer at an ice/water interface in the presence of turbulent flow have been treated by Gilpin *et al.* (1980). Alford and Carmack (1987) noted that the hydraulic resistance of the reach appeared to increase coincident with the onset of ripple formation.

To examine the evolution of these features over a period of time, several ice sections were cut out, overturned, spray-painted, and photographed. Typically, these observations (shown here as made at M, 30 m from the left bank) reveal a dramatic change in the nature of the ice/water interface in a very short period of time. Initially, the bottom of the ice is featureless (Fig. 27). Then, as solar radiation begins to penetrate the cover and warm the underlying water, ripples begin to form (Fig. 28). At first the ripples are essentially straight-crested. As the amplitudes of the ripples grow, they extract more energy from the flow and the crests become strongly undulated (Fig. 29). In the final stages the crests of the ripples become discontinuous and broken (Fig. 30) and thus cannot be traced over distances much longer than the wavelength. By this time the amplitudes are in the order of 5 cm.

DISCUSSION

General Patterns

Table 4 summarizes a comparison of some of the features observed in the winters of 1983/84 and 1984/85. In general, the winter of 1984/85 was characterized by higher air temperatures and greater snowfall than the previous one. In the second year of study, the date of breakup was later. Also in the second year, the ice was thinner and a lead remained open at Marwell throughout winter.

Based on these two years of observation, some preliminary remarks about the freeze-up and breakup patterns of the Yukon River at Whitehorse can be made.

(1) Freeze-up jams and ice bridging can occur in the narrows at X4, near the depot, and immediately above the Robert Campbell Bridge.

(2) Ice front advance is most rapid between BM and X2.

(3) Highest water levels occur during the time the ice front advances between M and AM.

(4) Open leads may persist through winter at M and immediately below the bridge.

(5) Breakup, while increasing the hydraulic resistance of the reach, has little effect on water level.

Table 4. Summary Comparison of the Winters of 1983/84 and 1984/85

Event	Winter 1983/84	Winter 1984/85
Date of ice front at BM	Dec. 4	Dec. 9
Date of ice front at M	Dec. 9	Dec. 13
Date of ice front at AM (defined as freeze-up)	Jan. 2	Dec. 29
Maximum ice thickness at M	1.0 m	0.7 m
Date of maximum ice thickness at M	Feb. 7	Mar. 19
Maximum percentage-area of frazil dam at M	41.6%	39.8%
Date of maximum percentage-area of frazil dam at M	Dec. 14	Feb. 12
Maximum water level at M	3.501 m	3.471 m
Date of maximum water level at M	Dec. 9	Dec. 16
Maximum water level at AM	4.812 m	5.085 m
Date of maximum water level at AM	Jan. 1	Dec. 30
Date of ice clear at White Pass Station	Mar. 22	Apr. 8
Date of ice clear at AM	Mar. 23	Apr. 8
Date of ice clear at M	Mar. 25	Apr. 10
Date of ice clear at BM (defined as breakup)	Mar. 29	Apr. 12
Snowfall from Nov. 1 to Mar. 31*	0.724 m	1.672 m

*Recorded by the Atmospheric Environment Service at Whitehorse.

Frazil Dam Formation

Our observations to date suggest that stream geometry influences frazil deposition so that frazil dams will form at the same location each year and will likely exhibit the same cross-sectional profile and area from year to year. Dams appear to grow in size until the cover stabilizes (immediately after freeze-up) and then gradually erode to breakup.

The composition of slush changes constantly through the season. It may appear as fine spicules and discs initially,

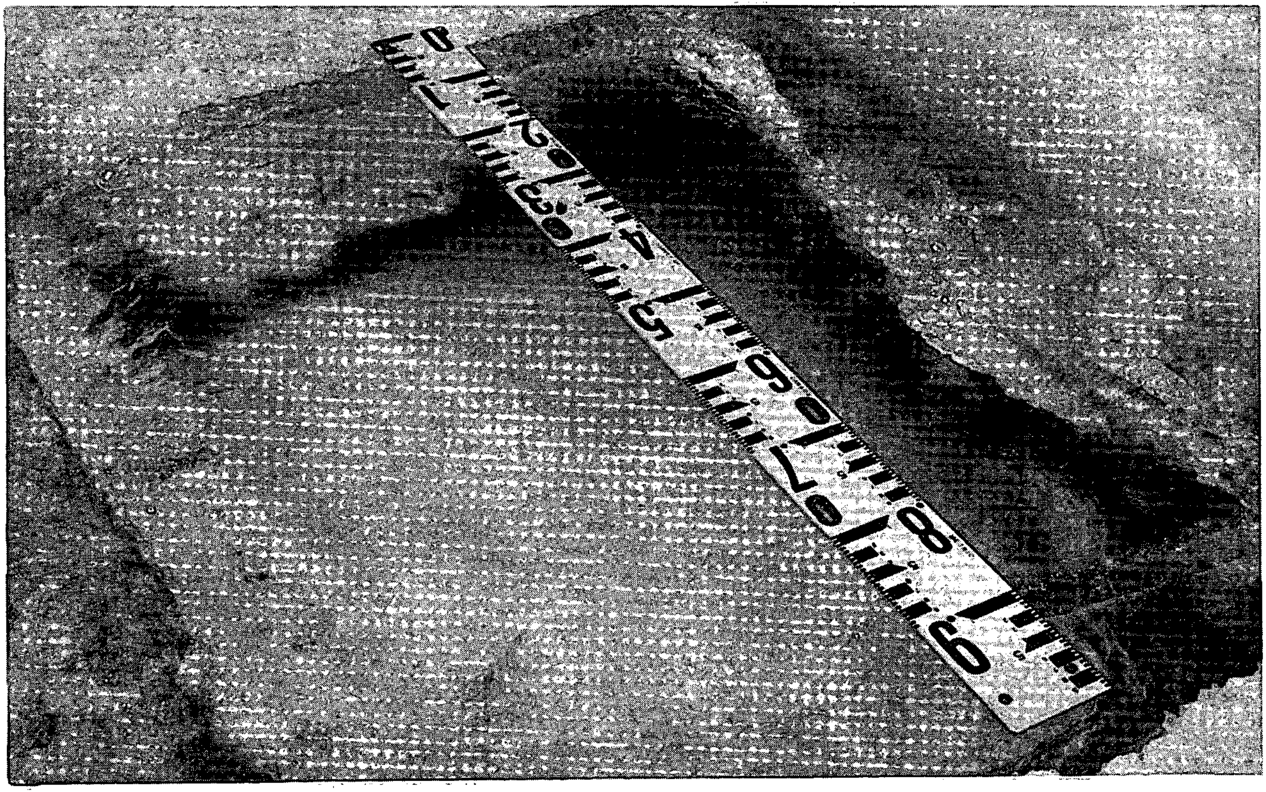

Figure 27. Bottom of ice showing no features (March 13, 1985).

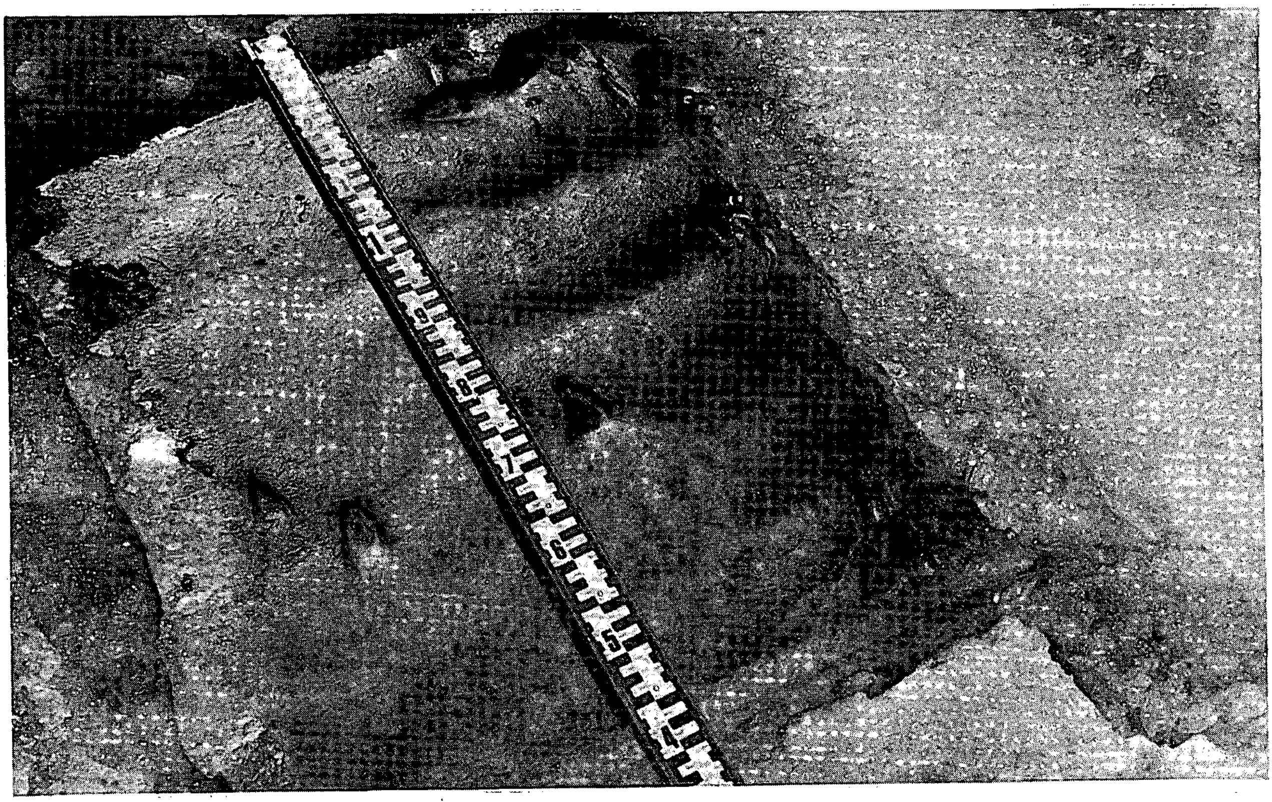

Figure 28. Ripples beginning to form (March 28, 1985).

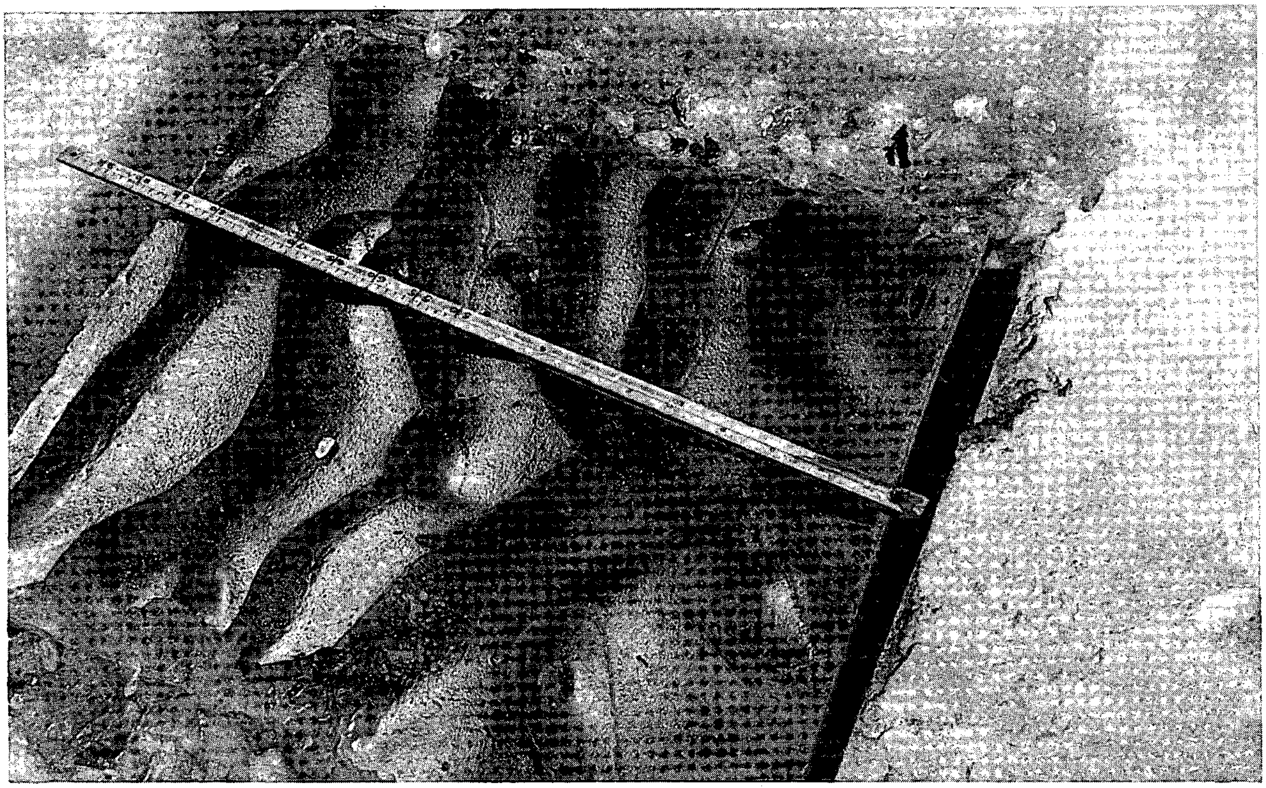

Figure 29. Crests becoming strongly undulated (April 2, 1985).

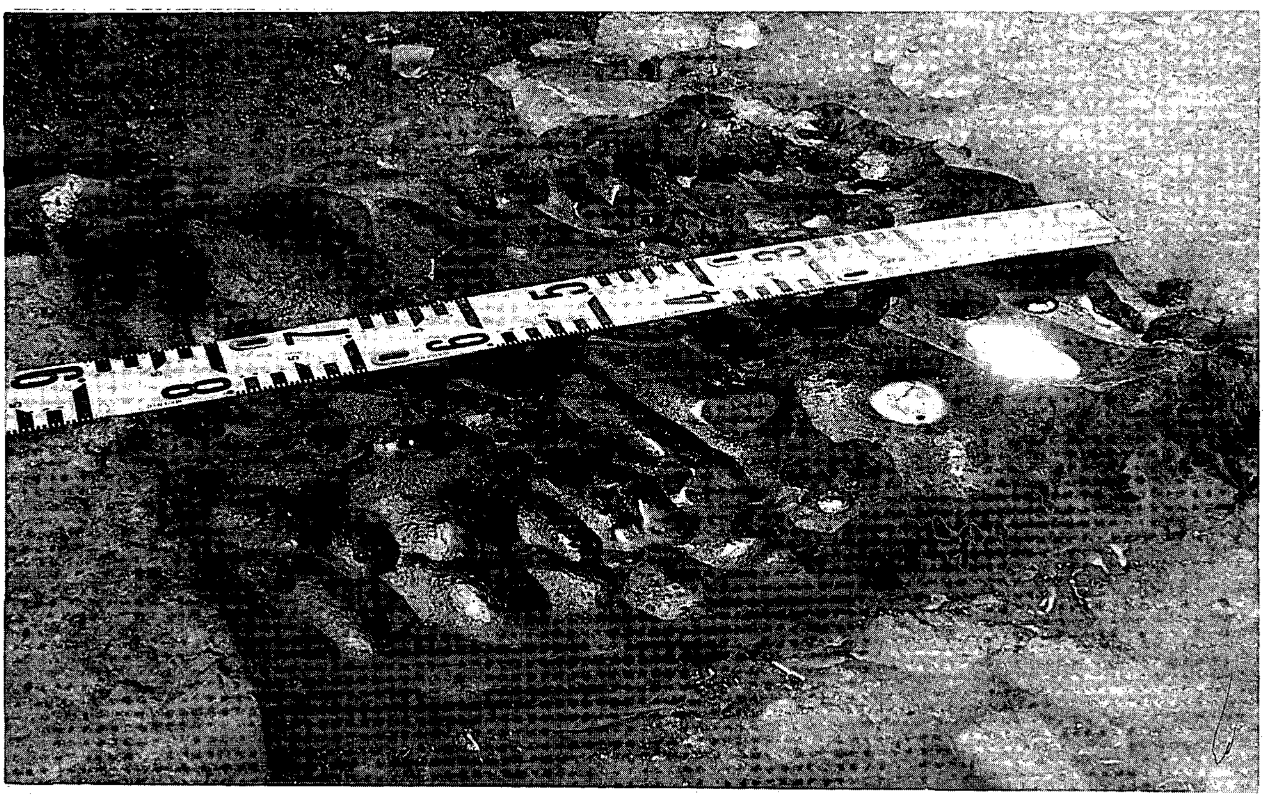

Figure 30. Crests becoming discontinuous and broken (April 8, 1985).

but change to nodules the size and shape of seagulls' eggs prior to breakup. The latter has also been reported by D. Lawson and E. Chacho (1985, U.S. Army, Corps of Engineers, Cold Regions Research and Engineering Laboratory; pers. com.). Also, there is vertical structure in frazil dams, with the slush having a maximum hardness about 1 m below the ice/slush interface.

Finally, we note there are two possible types of frazil deposition during the freeze-up period. First, lateral deposition, which occurs under shore ice; and second, medial deposition, which occurs under the last part of the section to freeze over, where the velocity is highest and the ice is roughest. It is the latter that may strongly affect the conveyance capacity of the channel.

ACKNOWLEDGMENTS

We would like to acknowledge the enthusiastic help of E. Marles and V. Chamberlain in the cold work of data collection and the tedious work of data reduction. We also thank M. Jarvis for her assistance in reading water levels.

Drafting and illustrating were ably done by B. Gordon of Gordon Enterprises, Vancouver.

Finally, we are grateful to the staff at the Whitehorse Rapids hydro site for providing streamflow data, and to Arctic Diamond Drilling Inc. in Marwell for allowing us daily passage through its property.

REFERENCES

Alford, M.E., and E.C. Carmack. 1987. Observations on ice cover and streamflow in the Yukon River near Whitehorse during 1983/84. NHRI Pap. No. 32, Sci. Ser. No. 152, National Hydrology Research Institute, Inland Waters/Lands Directorate, Environment Canada, Saskatoon, Sask.

Ashton, G.D., and J.F. Kennedy. 1972. Ripples on the underside of river ice covers. J. Hydraul. Eng., 98: 1603-24.

Carey, K.L. 1966. Observed configuration and computed roughness of the underside of river ice, St. Croix River, Wisconsin. U.S. Geol. Surv. Prof. Pap., 550-B: 192-98.

Gilpin, R.R., T. Hirrata, and K.C. Cheng. 1980. Wave formation and heat transfer at an ice-water interface in the presence of a turbulent flow. J. Fluid Mech., 99: 619-40.

Martin, S. 1981. Frazil ice in rivers and oceans. Annu. Rev. Fluid Mech., 13: 379-97.

Osterkamp, T.E. 1978. Frazil ice formation: a review. J. Hydraul. Eng., 104: 1239-55.

Osterkamp, T.E., and J.P. Gosink. 1983. Frazil ice formation and ice cover development in interior Alaska streams. Cold Reg. Sci. Technol., 8: 43-56.

Tsang, G. 1982. Frazil and Anchor Ice. National Research Council Subcommittee on Hydraulics of Ice Covered Rivers, Ottawa, Ont.

Appendix

Maps Illustrating the Advance and Retreat of the Seasonal Ice Cover During 1984/85

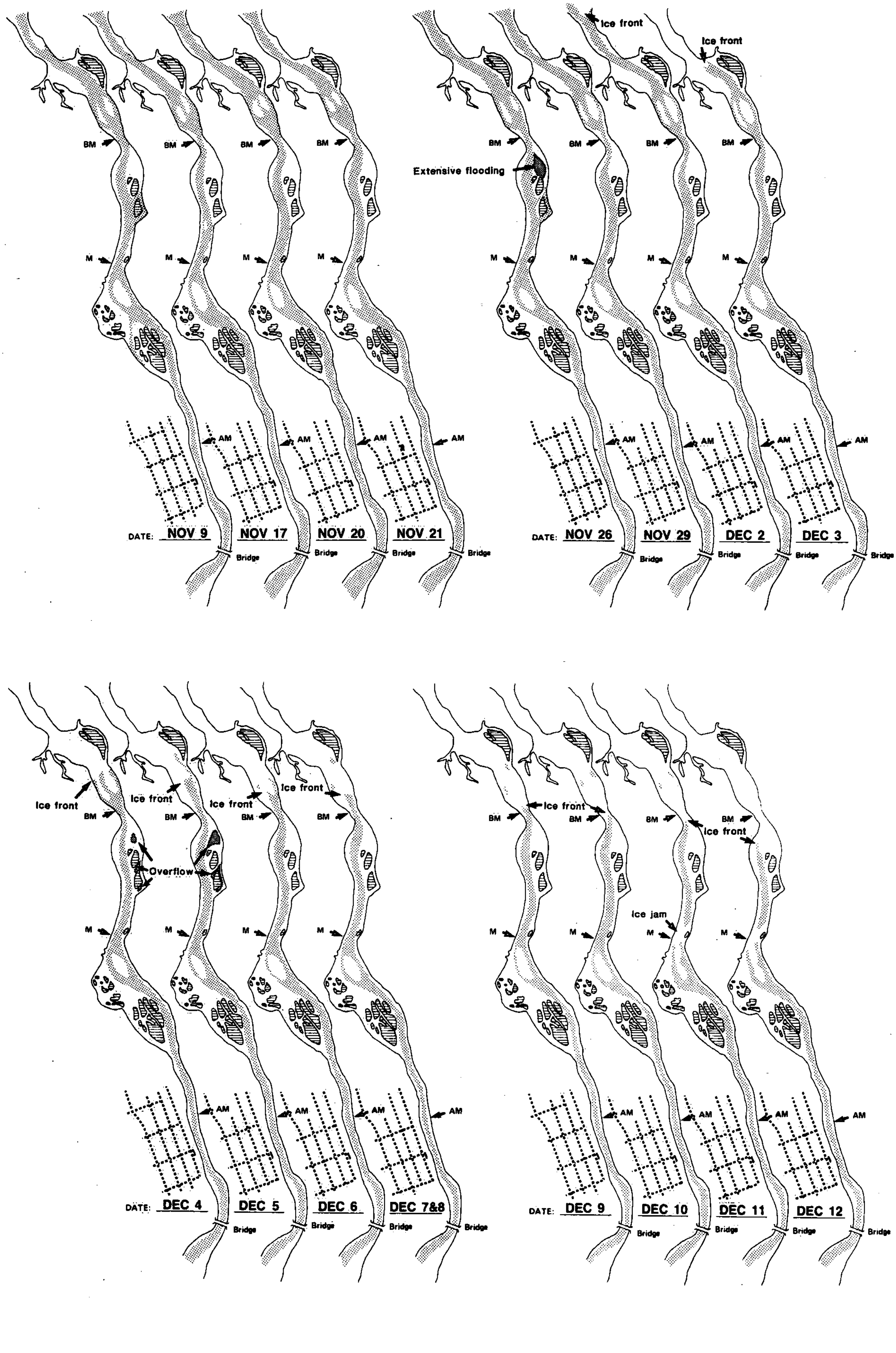

BM
M
AM
DATE: NOV 9
NOV 17
NOV 20
NOV 21
Bridge
Extensive flooding
Ice front
Ice front
DATE: NOV 26
NOV 29
DEC 2
DEC 3
Ice front
Ice front
Ice front
Ice front
Overflow
DATE: DEC 4
DEC 5
DEC 6
DEC 7&8
Ice front
Ice front
Ice jam
DATE: DEC 9
DEC 10
DEC 11
DEC 12

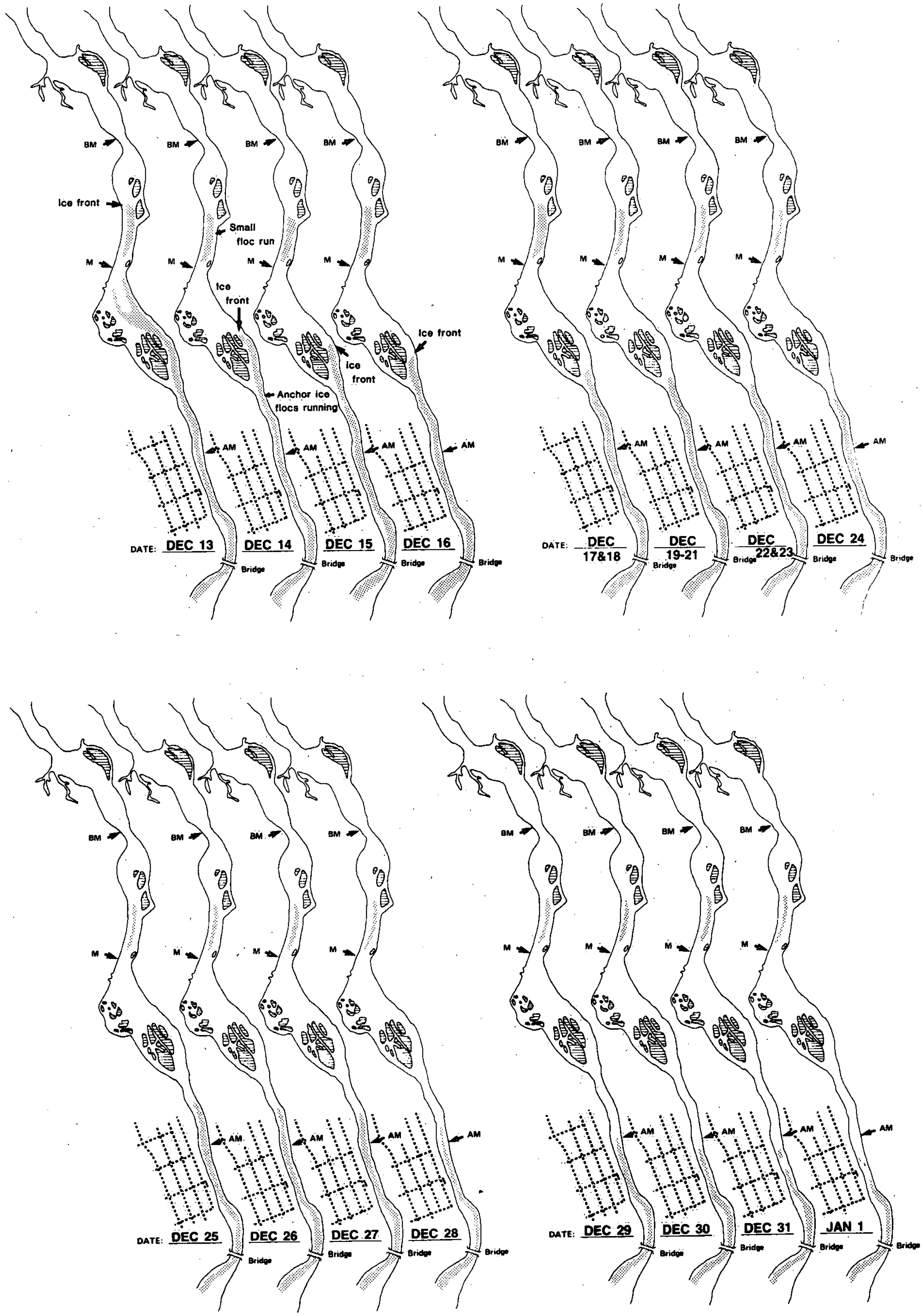
BM
Ice front
Small floc run
M
Ice front
Ice front
Ice front
Anchor ice flocs running
AM
DATE: DEC 13
DEC 14
DEC 15
DEC 16
Bridge
DATE: DEC 17&18
DEC 19-21
DEC 22&23
DEC 24
DATE: DEC 25
DEC 26
DEC 27
DEC 28
DATE: DEC 29
DEC 30
DEC 31
JAN 1

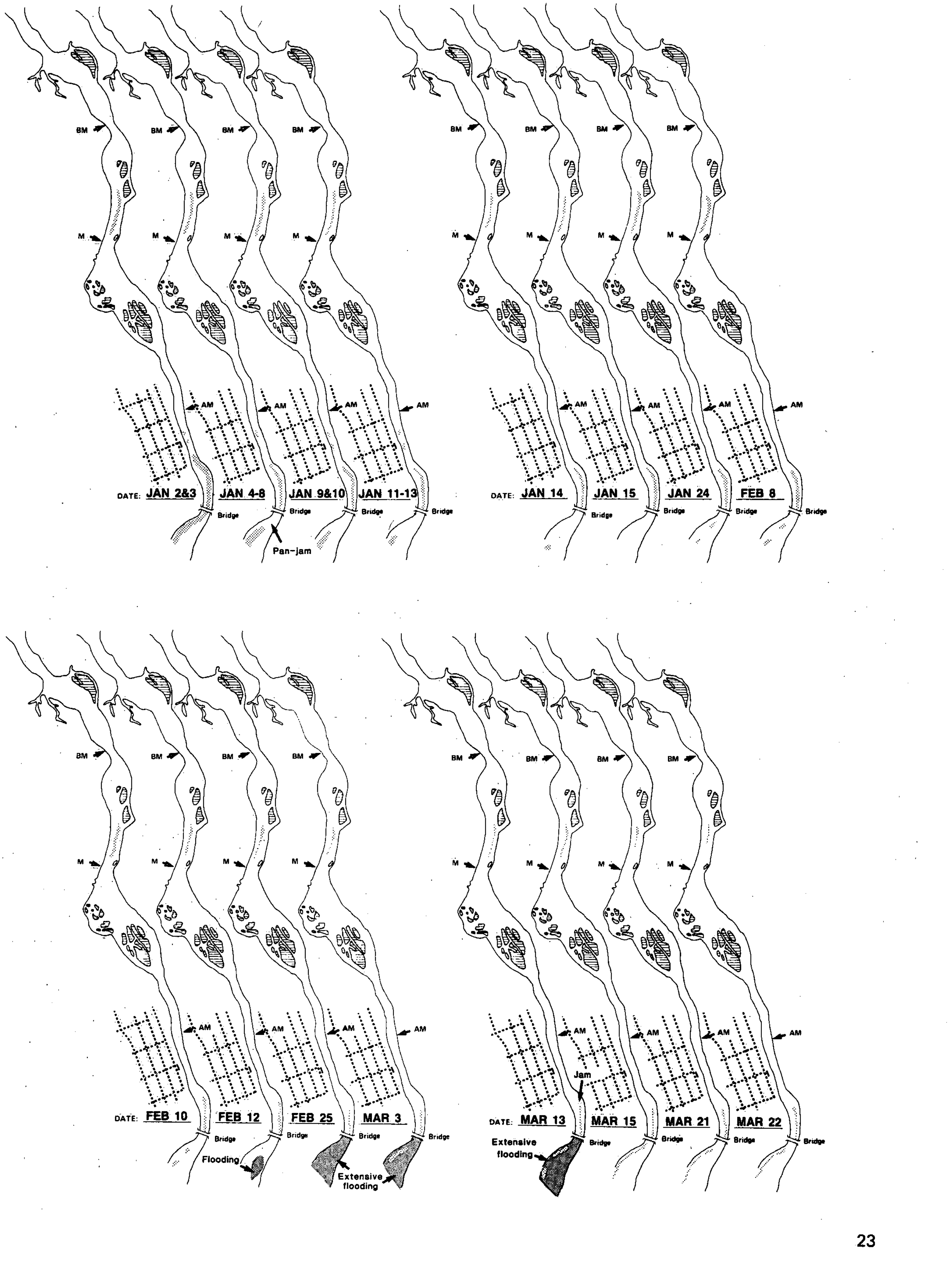
BM
M
AM
DATE: JAN 2&3
JAN 4-8
JAN 9&10
JAN 11-13
Bridge
Pan-jam
DATE: JAN 14
JAN 15
JAN 24
FEB 8
Bridge
DATE: FEB 10
FEB 12
FEB 25
MAR 3
Bridge
Flooding
Extensive flooding
DATE: MAR 13
MAR 15
MAR 21
MAR 22
Jam
Extensive flooding
Bridge

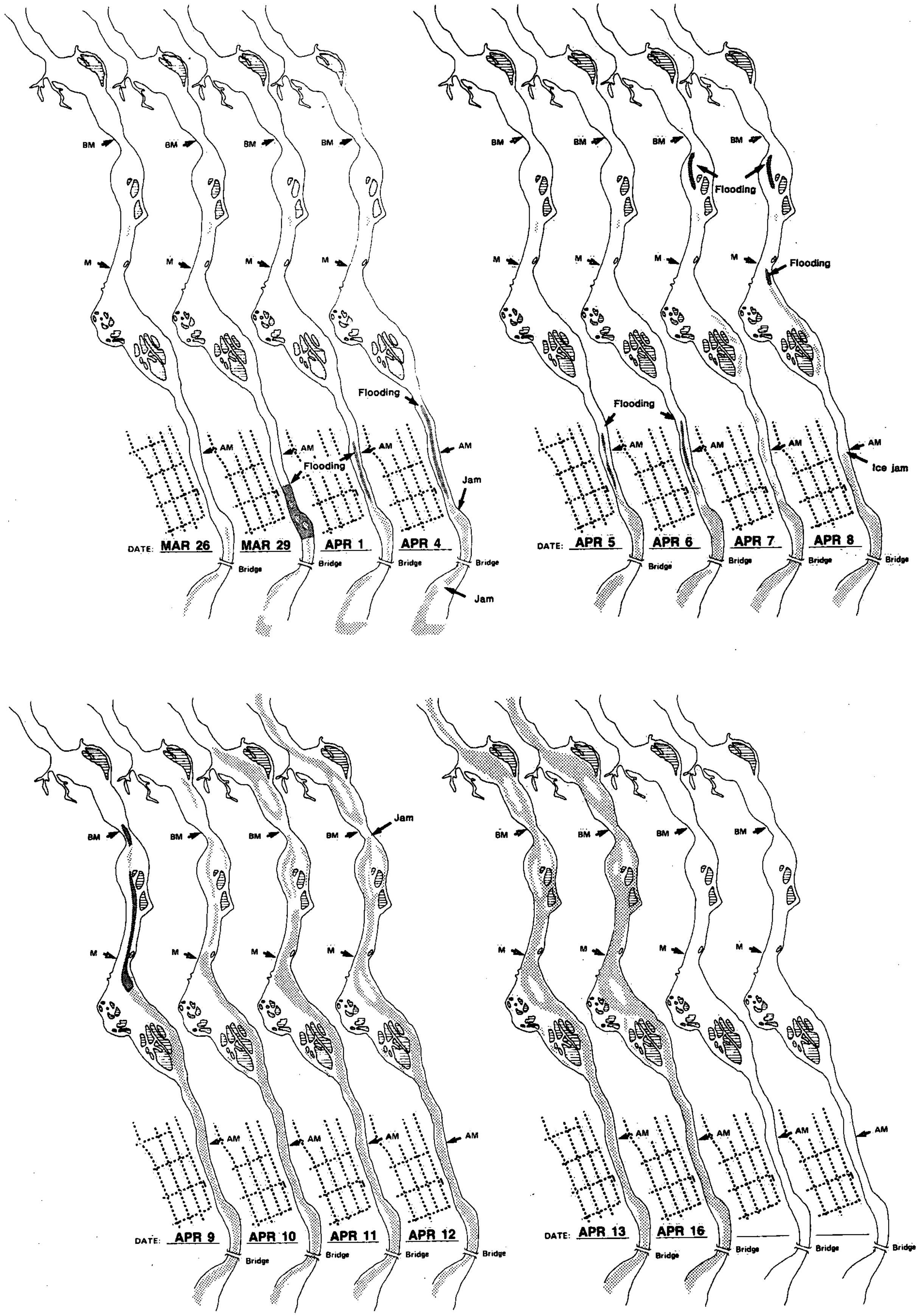

DATE:
MAR 26
MAR 29
APR 1
APR 4
BM
M
AM
Flooding
Flooding
Flooding
Jam
Jam
Bridge
DATE:
APR 5
APR 6
APR 7
APR 8
BM
M
AM
Flooding
Flooding
Flooding
Ice jam
Bridge
DATE:
APR 9
APR 10
APR 11
APR 12
BM
M
AM
Jam
Bridge
DATE:
APR 13
APR 16
BM
M
AM
Bridge

Canada